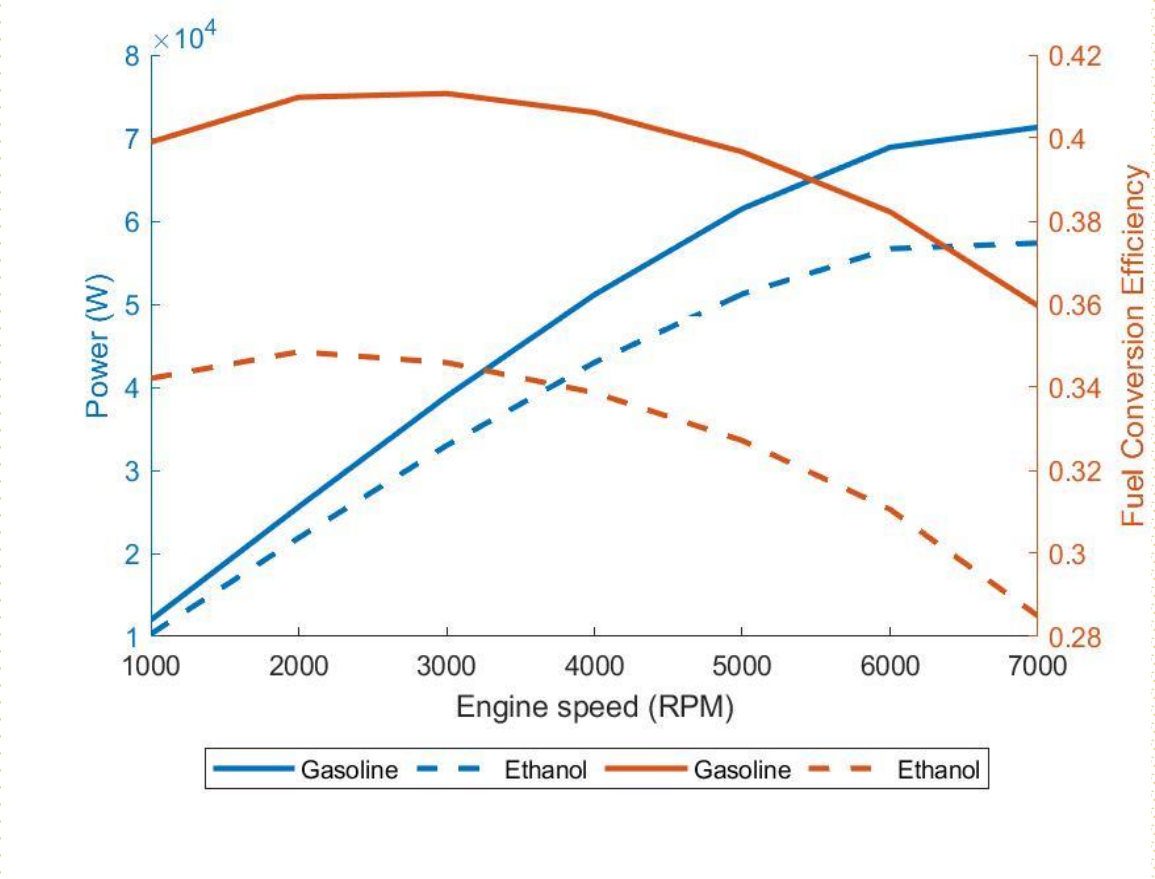

Pedro Alexandre de Castro Gonçalves

Cycle assessment of performance, specific fuel consumption and pollutant emissions of a four-stroke spark ignition ethanol fuelled engine

Dissertação de Mestrado em Energia para a Sustentabilidade
na Especialidade de Sistemas de Energia e Políticas Energéticas

• U C •

FCTUC FACULDADE DE CIÊNCIAS
E TECNOLOGIA
UNIVERSIDADE DE COIMBRA

DEPARTAMENTO DE
ENGENHARIA MECÂNICA

Cycle assessment of performance, specific fuel consumption and pollutant emissions of a four-stroke spark ignition ethanol fuelled engine

Submitted in Partial Fulfillment of the Requirements for the Degree of Master in Energy for Sustainability in the specialty of Energy Systems and Energy Policy

Avaliação do desempenho, consumo específico de combustível e emissão de poluentes do ciclo de um motor de quatro tempos de ignição por faísca utilizando etanol como combustível

Autor

Pedro Alexandre de Castro Gonçalves

Orientador

Pedro de Figueiredo Vieira Carvalheira

Júri

Presidente	**Professor Doutor Manuel Carlos Gameiro da Silva** **Professor Catedrático da Universidade de Coimbra**
Vogais	**Professor Doutor José Manuel Baranda Moreira da Silva Ribeiro** **Professor Auxiliar da Universidade de Coimbra**
Orientador	**Professor Doutor Pedro de Figueiredo Vieira Carvalheira** **Professor Auxiliar da Universidade de Coimbra**

Faculdade de Ciências e Tecnologia da Universidade de Coimbra

Coimbra, 1 de Julho,2020

“The meaning of the world is the separation of wish and fact.”

Kurt Gödel: as quoted in *The Outer Limits of Reason: What Science, Mathematics, and Logic Cannot Tell Us (MIT Press) 2013* by Yanofsky, Noson S.

Dedicado à minha família

Acknowledgements

This work was only possible due to the patience of my family and the collaboration and guidance of my supervisor, Pedro de Figueiredo Vieira Carvalheira, for which I am thankful.

Resumo

O objetivo desta tese de mestrado é melhorar a compreensão do funcionamento e operação dos Motores de Combustão Interna (MCI) pelo profissional do setor de energia. O resultado deste trabalho é um progama computacional capaz de simular a operação de um motor de combustão interna e prever a sua potência e consumo específico de combustível bem como a emissão de gases de efeito de estufa. O utilizador do programa apenas terá de introduzir especificações básicas sobre o MCI para obter resultados concretos e fiáveis em um curto intervalo de tempo.

A tese começa por introduzir os MCI e explicar a sua relevância, tanto a nível global como a curto, médio e longo prazo. De seguida, o modo de operação dos MCI é sucintamente descrito e os seus parâmetros principais identificados. Um modelo matemático baseado nos princípios físicos e químicos que regem o funcionamento do MCI é então construído e resolvido através de um programa de computador. O detalhe e o rigor da metodologia envolvida tanto na modelação matemática como na construção e execução do programa de computador servem como validação dos mesmos. Por último um conjunto de resultados é apresentado, interpretado e discutido.

Palavras-chave: Energia, Eficiência, Modelo, Computação, Motor de Combustão Interna, Etanol

Abstract

The purpose of this master's thesis is to improve the understanding of the function and operation of the Internal Combustion Engine (ICE) by the energy sector professional. The outcome of this work is a computer program capable of simulating ICE operation and predict its power output and specific fuel consumption as well as its Green House Gas emissions. The program user will only have to introduce basic ICE information to obtain concrete and reliable results in a narrow time span.

The thesis starts by introducing ICE's and explaining their relevance on a global scale as well as over short, medium and long term. Next ICE operation is succinctly described, and its main parameters identified. A mathematical model based on ICE physical and chemical working principles is constructed and solved through a computer program. The detail and thoroughness involved in the mathematical modelling, the programming and computation serve as model and computer program validation. Finally, a set of results from the program is presented, interpreted, and discussed.

Keywords Energy, Efficiency, Model, Computation, Internal Combustion Engine, Ethanol

Index

FIGURE INDEX

TABLE INDEX

Symbology

Roman letters

A_b	flame front area (m^2)
c_p	specific heat capacity at constant pressure (J/kg·K)
$\tilde{c}_p$	specific molar heat capacity at constant pressure (J/mol·K)
c_v	specific heat capacity at constant volume (J/kg·K)
$\tilde{c}_v$	specific molar heat capacity at constant volume (J/mol·K)
e	specific energy (J/kg)
h	specific enthalpy (J/kg)
$\tilde{h}$	specific molar enthalpy (J/mol)
m	mass (kg)
n	amount of matter (mol)
N	number of variables in system
	number of components in system
p	pressure (Pa)
Q	heat transferred (J)
s	piston location (m)
S_b	turbulent flame speed (m/s)
t	time (s)
T	temperature (K)
u	specific internal energy (J/kg)
$\tilde{u}$	specific molar internal energy (J/mol)
v	specific volume (m^3/kg)
$\tilde{v}$	specific molar volume (m^3/mol)
V	volume (m^3)
x_i	mole fraction of component i (mol/mol)
y_i	mass fraction of component i (kg/kg)

W work (J)

Greek Letters

θ crank angle (rad or °)

ρ density (kg/m^3)

τ ignition delay (s)

ϕ fuel-air mixture equivalence ratio

Constants

a crankshaft crank radius (m)

a_i coefficients to estimate thermodynamic properties

B cylinder bore (m)

L piston stroke length (m)

L_{cr} connecting rod length (m)

M molar mass (kg/mol)

ON octane number

R universal gas constant (J/mol·K)

R_i specific gas constant (J/kg·K)

Subscripts

b Burned Zone

ev exhaust valve

i system element

in transfer into the system

iv intake valve

out transfer out of the system

S system

u Unburned Zone

Abbreviations

ATDC	After Top Dead Centre
BDC	bottom dead centre
BTDC	Before Top Dead Centre
GHG	greenhouse gas
EV	electric vehicle
ICE	internal combustion engine
IEA	International Energy Agency
OECD	Organisation for Economic Co-operation and Development
R&D	research and development
RPM	rotations per minute
SI	international system (of units)
	spark ignition
TDC	top dead centre

1. INTRODUCTION

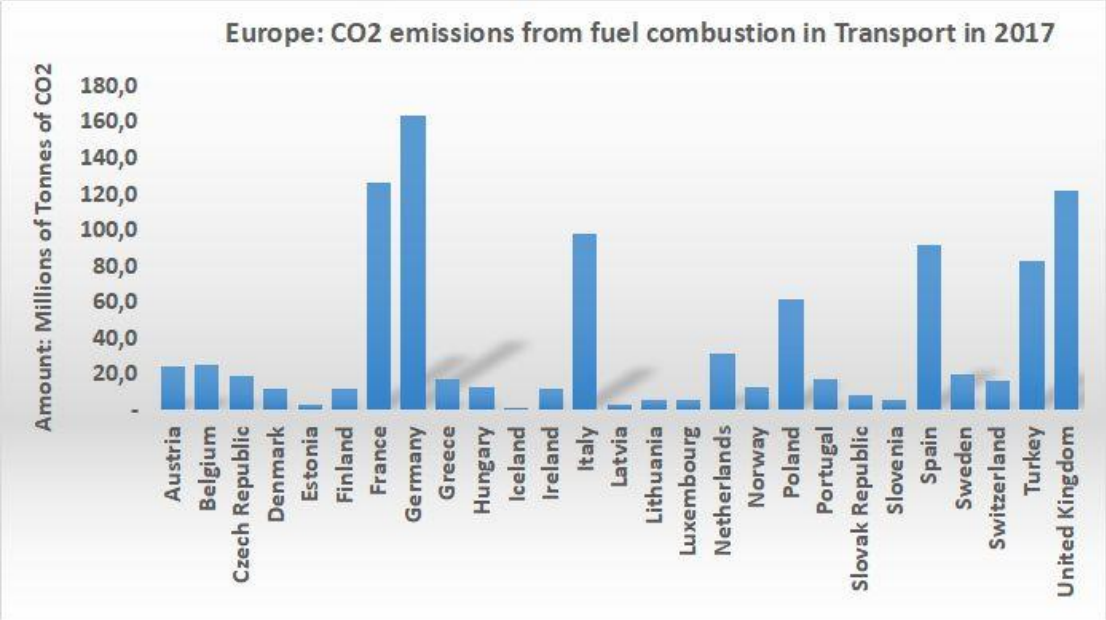

Figure 1: Transport based emissions in Europe in 2017 Based on IEA data from IEA 2019 CO_2 emissions from fuel combustion, IEA 2019, www.iea.org/statistics, All rights reserved; as modified by Pedro Gonçalves.

As can be seen from Figure 1 there are still significant CO_2 emissions occurring in transport in Europe, with France, Germany, Italy, the United Kingdom and Spain responsible for 60% of overall OECD European total in 2017. On a per capita basis, even a country like Denmark, which has pledged to renewable sources of energy, produced, through the use of transport, 5.75 kg of CO_2 per person per day on average in 2017, an amount higher than Germany or Portugal (Figure 2). (1) (2) (3)

In fact, as seen in Figure 2 (below), the per capita production of CO_2 in the sampled European countries is considerable, on average at 1915 kg per capita in 2017. Also noticeable is how European countries compare to African ones. Still from Figure 2 it can be seen that Denmark in 2017 produced 80× more CO_2 per capita than the Democratic Republic of Congo and the sampled European countries produced on average 4.6× the CO_2 of its

African counterparts. Overall, according to the IEA, in 2017, Africa produced 34% of the CO_2 emissions of OECD Europe. (1) (2) (3)

Taking into consideration the demographic and industrial or economic developmental trends of African and (extrapolating) worldwide countries it can be estimated, with confidence, that the impact of future CO_2 emissions will be considerable if there are no sustainable policies in action, such as diffusion, development and promotion of Energy Efficient technologies in transport.

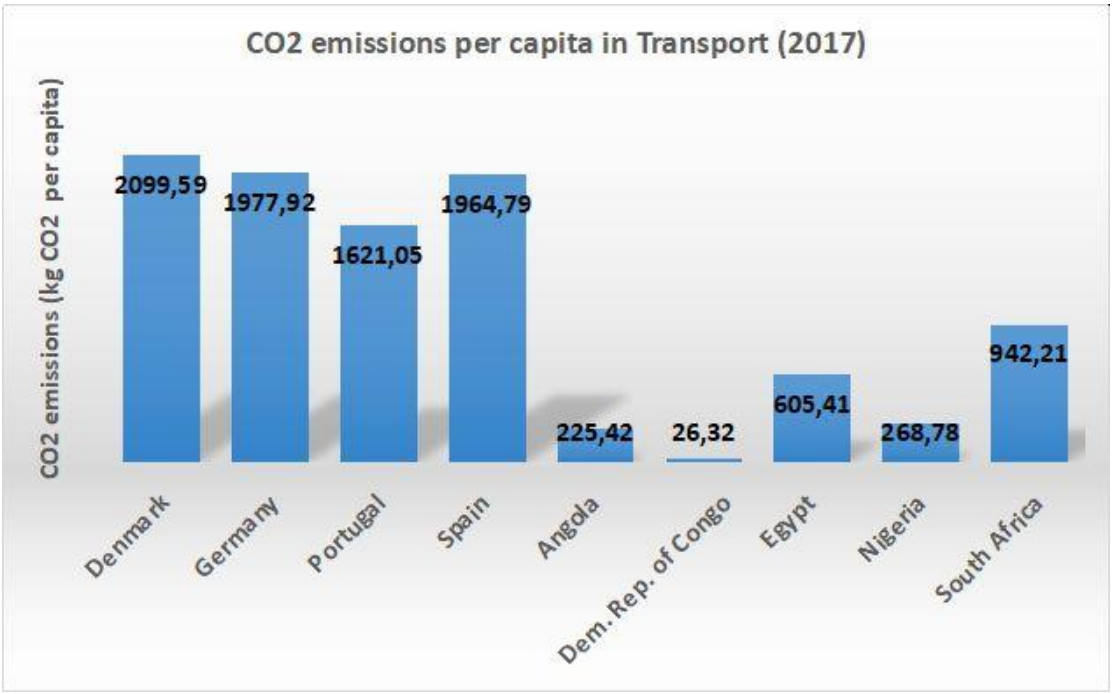

Figure 2: CO_2 emissions per capita in a sample of African and European countries. Based on IEA data from IEA 2019 CO_2 emissions from fuel combustion, IEA 2019, www.iea.org/statistics, All rights reserved; as modified by Pedro Gonçalves

As a single technology solving the entire problem (such as EV's) is completely unrealistic (1), two simple sustainable measures to mitigate CO_2 impact in transports are through the blending of biofuels - like ethanol - to existing CO_2 intensive fuels (like gasoline) or investing in R&D (modelling) of current existing transport technologies like the Internal Combustion Engine (ICE). This monograph describes a simple easy to use way to design and implement a model of an ICE, through the mathematical interpretation of engine

phenomena and posterior MATLAB program design. This model enables the prediction of engine efficiency, be it its drawbacks such as CO_2 production as well as its benefits, the generation of propulsive power and torque. All figures and results presented in this work are the result of model simulation of real ICE operation. (1) (2) (3)

1.1. Literature review

In order to construct a functional model of an internal combustion engine (ICE), a model that would allow prediction of its efficiency, on a first approach standard textbooks on internal combustion engines were consulted (4) (5) (6) (7).

(5) (8) present ICE's as first and foremost an organized machine, whose interconnected ordering of components strongly correlates with its efficiency. (4)'s main idea is that all phenomena in ICE's can be traced back to specific identifiable measurable processes and its respective parameters, even if ICE processes can be difficult to measure and highly nonlinear. (7) present and overview of the state of the art in modelling those processes, from the simplest 0D models to CFD based 3D ones.

Practical illustrations of ICE models were acquired mainly through the work of (9) (10) (11) (12). The effort of modelling an ICE as an energy system is based on first and foremost, defining the boundaries of such a model, in particular deciding upon the trade-off between degree of complexity desired (i.e. the amount of phenomena described by the model) and computational cost. In this work it was decided to construct the most complex model that could be implemented in a home computer (i.e., without the use of parallel processors) (10) (13).

The actual mathematical model is a translation of established ICE engine expertise, verified and based on well-established theoretical principles (4) (14) (15) (16) (17). The required data was obtained from trusted sources such as (18) (19) (20). Finally, the decision to use ethanol as ICE fuel was based on studies on fuel toxicity (21), renewable fuel potential (2) (22), as well as the increasing regulation and demands on fuel performance.

MATLAB (23) was chosen to be the computational simulation tool. It is accessible, rapidly expanding (Simulink tools imply worldwide collaboration) (13), quite powerful in its computational techniques (24) and it involves a supportive MATLAB user community.

1.2. Research gap

The conclusion drawn from the literature review was that ICE models and modelling codes are not widely available to a more general audience, e.g. from the perspective of a party interested in selecting energy efficient technologies without being an expert in the ICE field. Specific computational ICE modelling issues and methods are equally not mentioned, with (electric) power systems or aeronautical models being the main sources of information. That way this research work aims to plug this research gap through showcasing all the steps and stages of modelling the energy efficiency of an ICE, documenting the methodology used, highlighting its main parameters, including its issues and challenges and highlighting its benefits. (25) (26)

1.3. Dimensional analysis and nomenclature

The international system of units (SI) was used as the reference in this work being M (mass), T (time), L (length), Θ (temperature) and N (number of elementary particles) the fundamental dimensions. Dimensional analysis was used frequently throughout this work being a fast and simple way to check for errors.

To identify the thermodynamic system being modelled the symbol S is used, meaning the thermodynamic model is valid over a system S. This symbol can then become either u (for Unburned Zone) or b (Burned Zone), meaning the system being modelled is the Unburned or Burned Zones of the combustion process, respectively. (27)

2. ENGINE COMBUSTION SYSTEM

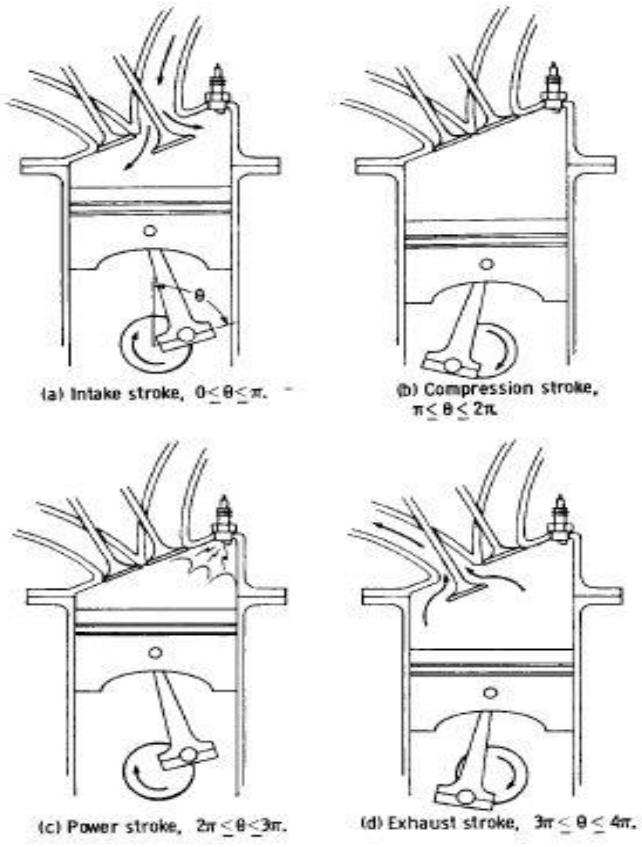

Figure 3: Engine Combustion System operation (9)

Intake valves control access of fresh mixture (premixed air and fuel) to a combustion chamber, which has the geometry shown in Figure 3. Connected to the base of the combustion chamber is a sliding piston, usually made of an aluminium alloy, which is attached through a crankshaft-connecting rod mechanism to a work producing shaft. There are also exhaust valves which control gas exhaust from the combustion chamber. All ICE systems are connected and synchronized, their coordination being key to its efficient operation. (4) (11)

Inside the combustion chamber, in the case of Spark Ignition (SI) engines, there is a spark plug device which, when activated, ignites the mixed air-fuel system. It is the expansion of the ignited air-fuel mixture (the working fluid) that causes the piston to move,

in a reciprocating way (from its top location, called Top Dead Centre (TDC) to its bottom one Bottom Dead Centre (BDC)), and to generate propulsive power. (4) (7)

The operation of SI engines is limited by its physical dimensions, its mechanics and the chemical processes involved in air-fuel premixed turbulent flame combustion. (4) (10) and (28)

2.1. Engine parameters

The engine specifications are:

- **number of engine cylinders**: in this work considered as 4;

- **cylinder diameter**: in this work considered as 0.075 m;

- **stroke length:** assumed to be 0.077 m;

- **connecting rod length**: valued at 0.14025 m;

- **compression ratio**: in this work takes the value of 10.5;[1]

- **rotational speed:** initially set at 6000 RPM.

The most relevant parameters in engine efficiency are:

- **fuel air mixture equivalence ratio**: the ratio between the fuel-air proportion used in engine operation and stoichiometric fuel-air proportion.

- **ignition timing**: the point in an engine's cycle when ignition occurs (expressed in crank angle before top dead centre, BTDC);

- **engine rotational speed**: the number of revolutions an engine performs in a period of time;

- **ignition delay**: a parameter linked to the occurrence of knock phenomena, abnormal combustion. (4) (29)

[1] Compression ratio is a relevant parameter in engine operation but was not studied in depth.

The main parameters involved in evaluating engine energy efficiency are: (4)

- **Torque**: the work delivered by the ICE per unit crank angle rotation.
- **Specific fuel consumption**: measuring the rate of conversion of fuel onto power produced.
- **Engine power**: the power transferred from the working fluid to the piston.
- **Pollutant emissions**: the amount of CO_2 and pollutant gases emitted during ICE operation (usually evaluated on a cycle or gases emitted volume fraction basis).

2.2. Crank angle and piston location

An engine combustion system's processes are usually expressed in terms of crank angle (evaluated at degrees or radians) (10). The conversion of the engine's translational motion (given by piston location) onto the engine's rotational motion (given by crank angle) is achieved through by Eq. (2-1) (4):

$$s = a \times \cos(\theta) + \left[{L_{cr}}^2 - [a \times \sin(\theta)]^2\right]^{1/2} \quad (2\text{-}1)$$

Where *s* is piston location given by the distance between the crankshaft rotation axis and the piston pin axis, *a* is crankshaft crank radius, L_{cr} is connecting rod length and θ is crank angle. Two valves, one intake and one exhaust, control access to the engine combustion system. Gas flow driving force is the pressure difference between intake or exhaust port and the inside of the cylinder: a favourable pressure difference drives mass from the port into the system and an unfavourable difference will drive mass from the engine combustion system onto the intake or exhaust ports. (4) (11) (16)

Figure 4 shows the lift (a measure of the valve's opening) of the intake valve (in m) as a function of crank angle. As shown, the intake valve opens at the end of the cycle at 698.5° (the engine cycle is considered to start at top dead centre), achieving a maximum opening of 8.2 mm at around 105º crank angle. The intake valve closes at 241° crank angle.

2.3. Intake and exhaust valves

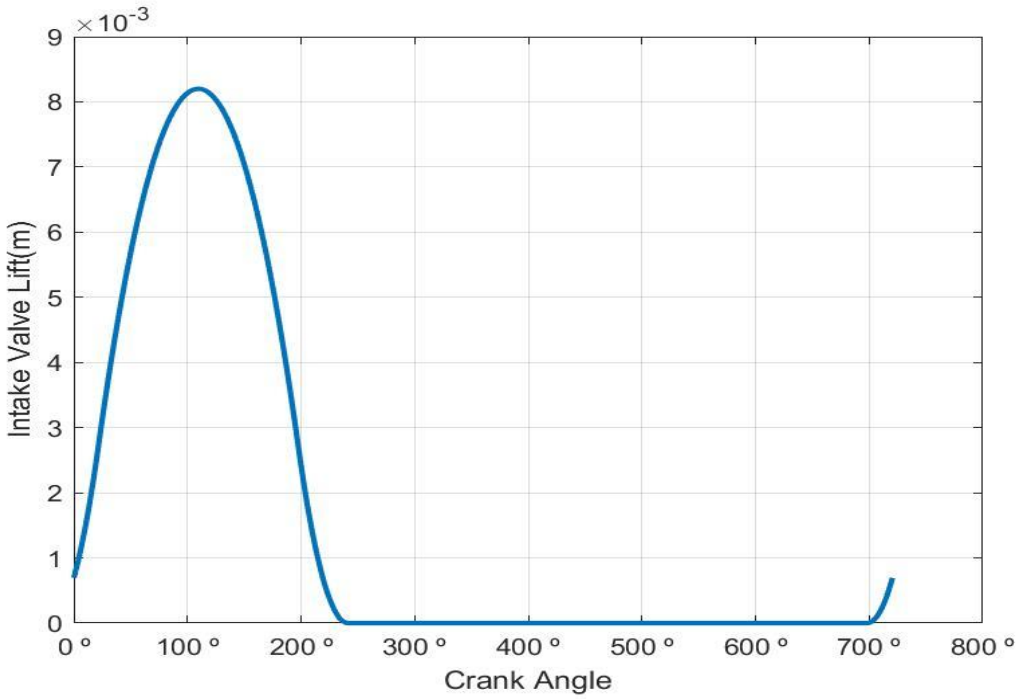

Figure 4: Intake valve lift as a function of crank angle (measured at 6000 RPM and ignition timing 35º BTDC)

2.4. Molar mass

A key parameter in these calculations is molar mass, be it of each individual species of the system, of fresh mixture, of burned gases, of each zone or of burned residual gases, as it enables the conversion from molar to mass base. System molar mass is a partial property (15) and its rate of variation with time can be related to individual mole fraction variation with time, (2-2):

$$\left(\frac{dM}{dt}\right)(t) = \left(\sum_{i=1}^{N} M_i \frac{dx_i}{dt}\right)(t) \qquad (2\text{-}2)$$

Where M is system molar mass, M_i is component i molar mass and x_i is component i mole fraction. An equally useful expression enables the calculation of system molar mass given its component individual molar masses and mass fractions, y_i: (5)

$$M = \left[\sum_{i=1}^{N} \frac{y(i)}{M_i}\right]^{-1} \quad (2\text{-}3)$$

2.5. Estimation of thermodynamic properties

Specific heat capacity and enthalpy are given by empirical equations. The empirical equations given for fitting specific heat has the form: (19)

$$\frac{c_p(T)}{R} = \sum_{i=1}^{r} a_i T^{q_i} \quad (2\text{-}4)$$

Where $c_p(T)$ is specific heat capacity, R is the universal gas constant, a_i are empirical coefficients and T^{q_i} terms which are functions of temperature.

2.6. Combustion

The oxidation-reduction reaction involved in combustion is:

$$\mathrm{C}_a\mathrm{H}_b\mathrm{N}_c\mathrm{O}_d + x\left(\mathrm{O}_2 + Z_{\mathrm{N}_2}\mathrm{N}_2 + Z_{\mathrm{Ar}}\mathrm{Ar}\right) \rightarrow e\mathrm{CO}_2 + f\mathrm{H}_2\mathrm{O} + g\mathrm{N}_2 + h\mathrm{Ar}$$

Where *a*, *b*, *c* and *d* define the atomic composition of the fuel molecule. *x* is the stoichiometric proportion of air to fuel in the reaction and *e*, *f*, *g* and *h* are the amounts of products yielded by one molecule of fuel (26).

The equivalence ratio is given by:

$$\phi = \frac{\#\mathrm{Oxygen}_{\mathrm{oxidize}}}{\#\mathrm{Oxygen}_{\mathrm{mixture}}}$$

The numerator expresses the oxygen content (the number of oxygen atoms) required to fully oxidize the air-fuel mixture. The denominator expresses the oxygen content (the number of oxygen atoms) in the air-fuel mixture. (2) (4)

3. THEORETICAL MODEL

A theoretical model was developed under the following approach: (4) (7) (24) (30)

- **objective**: the objective of the model is to predict system behaviour over time (as expressed in crank angle).

- **system design**: *N* variables of interest (i.e. the system's degrees of freedom to be explained) are defined.

- **system behaviour**: an equal *N* number of constraints were found, so as to define system behaviour. Constraints were based on assumptions, physical and chemical principles (conservation laws) and empirical formulas.

- **system test**: in order to test the system for robustness model system response to variation in model parameters was studied.

The model is 0-Dimensional, assumes all intensive variables are uniform (there are no spatial gradients) and considers the existence of two zones during the combustion. One zone, in this monograph labelled Unburned Zone, is comprised of the mixture of air and fuel as well as leftover residual burned gases. The other, comprised of burned gases is here labelled Burned Zone. A reaction flame constitutes the interface between these two zones and phenomena such as flame quenching or wall interaction are not considered. (9) (10)

Finally, no heat transfer occurs between Unburned and Burned Zones and the work required to transfer fluid from the unburned zone to the burned zone is negligible. Both zones are modelled as two distinct but interacting thermodynamic systems. (10) (26)

3.1. Variable definition

The engine combustion system variables were grouped onto six classes, the first one containing the independent variables (time), the second class containing state variables and the final one key parameters: (7) (26)

- **time**: process variables are expressed according to time (crank angle is directly proportional to time as engine rotational speed is assumed constant).

- **pressure**: of Burned or Unburned Zone.

- **volume**: of Burned or Unburned Zone.

- **mass**: of each system species: on a first approach the system species are fuel, air (oxygen, nitrogen and argon) as well as carbon dioxide and water. On a second approach the system includes also carbon monoxide, hydrogen (molecule), hydrogen (atomic), oxygen (atomic), oxygen hydroxide, nitrogen monoxide and nitrogen (atomic).

- **temperature**: the temperature of Burned and Unburned Zone.

- **mole fractions**: the mole fractions of all components in Burned Zone.

- **flame variables**: variables describing flame behaviour.

- **knock**: a parameter to evaluate knock occurrence. (4)

3.2. Stages

The engine's operation has been divided in five different stages. The motivation for this is that the model in each stage is uniform. The titles of the each stage and respective processes are: (4) (30)

"Intake and Compression" stage:

- starts when exhaust valve closes and ends at ignition timing.

- includes fresh mixture and burned residual gases inlet process (through the intake system).

- includes compression process.

- an intake manifold is considered.

- the system is assumed to be in Unburned Zone.

“Combustion” stage:

- this stage starts at ignition timing and ends when Unburned Zone fuel mass is zero.

- the combustion of the fuel-air mixture takes place.

- an interface comprised of a flame front separates an Unburned Zone (as defined in section 3) from a Burned Zone one. The Unburned Zone is composed of residual burned gases and an air-fuel mixture. The Burned Zone is created as the Unburned Zone is consumed.

- on a first approach Burned Zone composition is fixed and on a second approach it is considered to vary.

“Expansion and Exhaust” stage:

- this stage starts when the combustion stage fuel reaches zero and ends when the intake valve opens.

- the Burned Zone experiences an expansion process.

- burned gases leave through the exhaust port.

- the system is assumed to be in Burned Zone.

“Crossflow before top dead centre (BTDC)”:

- This stage starts when intake valve opens (before top dead centre, BTDC) and ends at top dead centre (TDC)

- As intake and exhaust valves are open gases flow from the system through the intake and exhaust ports and from the ports into the system.

- the system is still considered to be in Burned Zone.

"Crossflow after top dead centre (ATDC)":

- This stage starts at TDC (which is considered the start of the engine cycle) and ends when exhaust valve closes.

- equally there is outbound flow from the system through exhaust and intake ports and inbound flow from intake and exhaust ports into the system.

- system is assumed to be in Unburned Zone

3.3. Equation for pressure variation

The variation of system pressure is expressed through the Ideal Gas Law, which is a reasonable assumption as the system operates at high temperature and the molecular or atomic species involved are small: (15) (26)

$$(pV)_S = (nRT)_S \tag{3-1}$$

Where p is the system pressure, measured in (Pa), V is the system volume, measured in (m^3), n is the amount of matter in the system, measured in mol, R is the universal gas constant (J/mol·K) and T is the system temperature, measured in (K).

Using the notion of molar mass (Section 2.4) to convert n onto m the differential of system pressure evaluated at time t is expressed implicitly as, Eq.(3-2):

$$V_S dp_S(t) + p_S dV_S(t) - T_S \sum_{i=1}^{N} R_i dm_{i,S}(t) - \sum_{i=1}^{N} m_{i,S} R_i dT_S(t) = 0 \tag{3-2}$$

This equation means that in order to estimate system pressure $N+2$ degrees of freedom are involved. (15) Reordering the equation (order: p, V, m, T), dividing by V and correlating pressure with time variation a rate equation for pressure is obtained, Eq. (3-3):

$$\left(\frac{dp}{dt}\right)_S(t) + \frac{p}{V}\left(\frac{dV}{dt}\right)_S(t) - \left[\frac{T}{V}\sum_{i=1}^{N} R_i \frac{dm_i}{dt}\right]_S(t) - \left[\frac{1}{V}\frac{dT}{dt}\sum_{i=1}^{N} m_i R_i\right]_S(t) = 0 \quad (3\text{-}3)$$

It is of note that the subscript *s* (system) can refer to Unburned *u* or Burned Zone, *b*. (15)

3.4. Equation for volume variation

The total volume of the cylinder, V, is given by Eq. (3-4) and is the sum of Unburned Zone volume, V_u, and Burned Zone volume, V_b. (4)

$$V = V_u + V_b \quad (3\text{-}4)$$

Differentiating Eq. (3-4) with respect to time at time *t*:

$$\left(\frac{dV}{dt}\right)_S(t) = \left(\frac{dV_u}{dt}\right)(t) + \left(\frac{dV_b}{dt}\right)(t) \quad (3\text{-}5)$$

The time derivative of the total volume of the cylinder relates to the time derivative of s by Eq. (3-6). In Eq. (3-6) s is the distance between the crankshaft rotation axis and the piston pin axis, and B is the cylinder bore: (4)

$$\left(\frac{dV}{dt}\right)_S(t) = -\frac{\pi}{4}B^2\left(\frac{ds}{dt}\right)_S(t) \quad (3\text{-}6)$$

3.4.1. Equation for Unburned Zone volume variation

Eq. (3-7) correlates the time derivative of total system volume with combined derivatives of Unburned and Burned Zone volumes, respectively.

$$\left(\frac{dV}{dt}\right)_u(t) + \left(\frac{dV}{dt}\right)_b(t) = -\frac{\pi}{4}B^2\left(\frac{ds}{dt}\right)_S(t) \quad (3\text{-}7)$$

Which provides an equation for Unburned Zone volume variation over time.

3.4.2. Equation for Burned Zone volume variation

To express Burned Zone volume variation in terms of other system variables the specific gas constant ($R_i = \frac{R}{M_i}$) is used as well as the assumption that the Burned Zone and Unburned Zone pressure is the same due to considering the flame as a deflagration combustion wave, Eq. (3-8). (4)

$$p_S = \frac{\sum_{i=1}^{N} m_i R_i T_S}{V_S} \wedge p_u = p_b \Leftrightarrow \frac{\sum_{i=1}^{N} m_i R_i T_u}{V_u} = \frac{\sum_{i=1}^{N} m_i R_i T_b}{V_b} \tag{3-8}$$

Differentiating Eq. (3-8) with regards to time:

$$\begin{aligned} &\left[\left(\frac{T}{V^2}\sum_{i=1}^{N} m_i R_i \frac{dV}{dt}\right)_b - \left(\frac{T}{V^2}\sum_{i=1}^{N} m_i R_i \frac{dV}{dt}\right)_u\right](t) \\ &+ \left[\left(\frac{1}{V}\sum_{i=1}^{N} m_i R_i \frac{dT}{dt}\right)_u - \left(\frac{1}{V}\sum_{i=1}^{N} m_i R_i \frac{dT}{dt}\right)_b\right](t) \\ &+ \left[\left(\frac{T}{V}\sum_{i=1}^{N} R_i \frac{dm_i}{dt}\right)_u - \left(\frac{T}{V}\sum_{i=1}^{N} R_i \frac{dm_i}{dt}\right)_b\right](t) = 0 \end{aligned} \tag{3-9}$$

Which is the equation for Burned Zone volume variation. It is noted that this equation implies N_u+N_b+3 degrees of freedom. (15)

3.5. Equation for mass variation

System mass variation is expressed through the principle of mass conservation. On a first approach, the mass balance is: (15)

$$\begin{aligned} dm_s(t) &= dm_{in}(t) - dm_{out}(t) \\ &= dm_{in,iv}(t) + dm_{in,ev}(t) - dm_{out,iv}(t) - dm_{out,ev}(t) \end{aligned} \tag{3-10}$$

where dm_{in} and dm_{out} are the mass transferred into the system and out of the system, respectively, transfers which can be through intake or exhaust valves.

3.5.1. Combustion stage

For the combustion stage, the system total mass differential is: (4) (15)

$$dm_s(t) = dm_u(t) + dm_b(t) \tag{3-11}$$

Where m_u refers to Unburned Zone mass and m_b refers to the Burned Zone mass. This translates to a mass rate variation of:

$$\frac{dm_s}{dt}(t) = \frac{dm_u}{dt}(t) + \frac{dm_b}{dt}(t) = 0 \tag{3-12}$$

Considering Burned Zone mass creation depends on flame front area and speed as flame propagation is the only mechanism to both consume Unburned Zone mass and create Burned Zone mass and that the Unburned Zone has fixed composition:

$$\frac{dm_b}{dt}(t) = \rho_u S_b A_b \wedge \frac{dm_{i,u}}{dt}(t) = y_{i,u}\frac{dm_u}{dt} \Rightarrow \frac{dm_{i,u}}{dt}(t) = -y_{i,u}\frac{dm_b}{dt} \tag{3-13}$$

where m_b is Burned Zone mass, m_u is Unburned Zone mass, $y_{i,u}$ is the mass fraction of component i of the unburned gas, ρ_u is the density of the unburned gas, S_b is the flame speed and A_b is the flame front surface area. (4) (15)

Figure 5 illustrates how CO_2 mass flow rate during CrossflowBTDC stage varies with crank angle. It can be observed that the intake valve opens at around 700º crank angle but as system pressure is greater than intake or exhaust port pressures CO_2 flows out of the system onto the intake and exhaust ports. The CO_2 mass flow rate to the exhaust decreases steadily until 720º+20.8º when exhaust valve closes. Furthermore, it can be observed that after initially increasing, the CO_2 mass flow rate onto the intake valve decreases, driven by a decrease in system pressure.[2] (16)

[2] The pressure at both at intake and exhaust ports is 1 atmosphere. The discharge coefficients for intake and exhaust valves are the same.

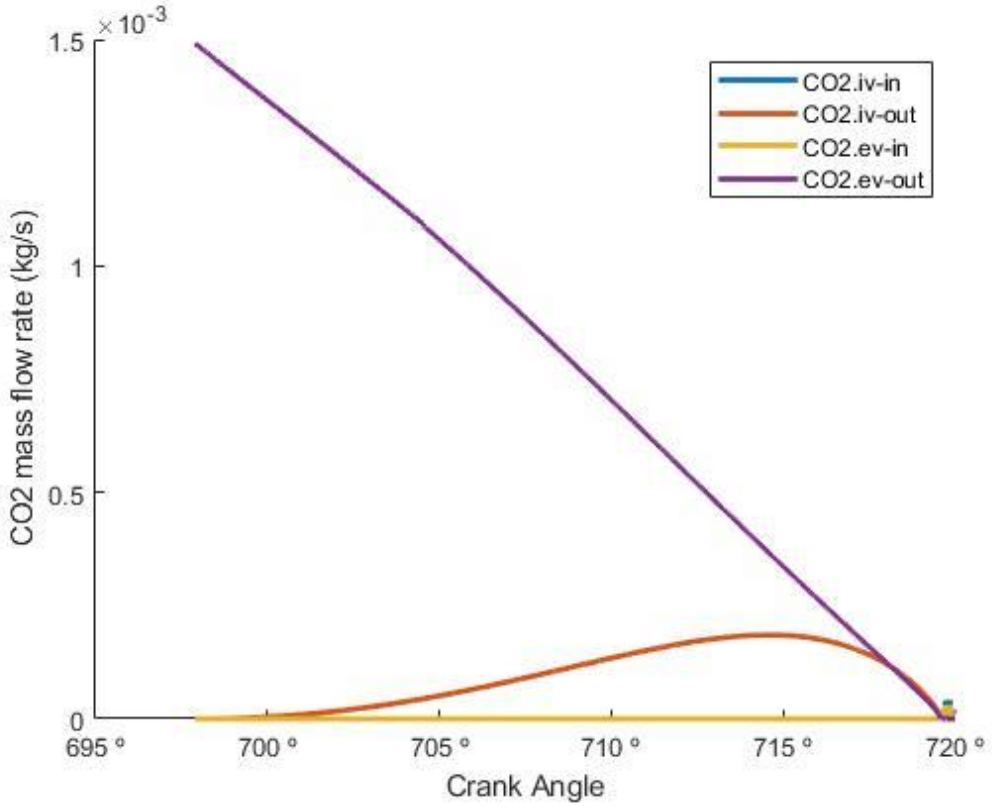

Figure 5: CO_2 mass flow rate at crossflow BTDC stage. “iv-in”: inflow into system through intake valve. “iv-out”: outflow from system through intake valve. “ev-in”: inflow into system through exhaust valve. “ev-out”: outflow from system through exhaust valve.

3.6. Equation for temperature variation

The engine combustion system’s temperature variation is expressed through an energy balance. The system’s energy is defined by the differential variation of system energy: (15)

$$d[E]_S(t) = d[m \times e]_S = [mde]_S + [edm]_S = [mdu]_S(t) + [udm]_S(t) \quad (3\text{-}14)$$

Where E_S is extensive system energy, e_S is intensive system energy, m_s is system mass and u_S refers to system internal energy. In this model system energy is estimated by internal

energy only as kinetic and potential energy are of a lower order of magnitude. Expanding upon the terms:

$$[du]_S(t) = [c_v dT]_S(t) \wedge u = h - pv \wedge [pv]_S(t) = \left[\sum_{i=1}^{N} y_i R_i T\right]_S (t) \tag{3-15}$$

The overall energy balance of the system is

$$d[E]_S(t) = [dE_{in} - dE_{out} + \delta Q - \delta W]_S(t) \tag{3-16}$$

where δQ is heat transferred from the surroundings to the system and δW is work done by the system onto the piston. Taking in consideration Eq. (3-15):

$$\begin{aligned}[mc_v dT]_S(t) = &\left[\sum_{i=1}^{N} (y_i R_i T)\frac{dm}{dt}\right]_S (t) + \left(\frac{\delta Q}{dt}\right)_S - \left(\frac{\delta W}{dt}\right)_S \\ &+ [(h_{in} - h_S)dm_{in}](t) + [(h_S - h_{out})dm_{out}](t)\end{aligned} \tag{3-17}$$

which is the energy balance final form. Correlating with time variation the equation for temperature variation is obtained:

$$\begin{aligned}\left[mc_v \frac{dT}{dt}\right]_S (t) = &\sum_{i=1}^{N} \left[(y_i R_i T)\frac{dm}{dt}\right]_S + \left(\frac{\delta Q}{dt}\right)_S - \left(\frac{\delta W}{dt}\right)_S \\ &+ \left[(h_{in} - h_S)\frac{dm_{in}}{dt}\right] + \left[(h_S - h_{out})\frac{dm_{out}}{dt}\right]\end{aligned} \tag{3-18}$$

3.6.1. Combustion stage

For the combustion stage the model in Eq. (3-18) is adjusted to become: (4)

$$\begin{aligned}\left[mc_v \frac{dT}{dt}\right]_b (t) = &\sum_{i=1}^{N} \left[y_i R_i T \frac{dm}{dt}\right]_b (t) + \dot{Q}_b - \dot{W}_b \\ &+ \left[(h_u - h_b)\frac{dm_{in}}{dt}\right](t)\end{aligned} \tag{3-19}$$

Where the index *b* refers to Burned Zone and index *u* refers to Unburned Zone.

The model is interpreted the following way (15) (17) (26):

Table 1: Interpretation of energy equation terms

$\sum_{i=1}^{N} m_i c_{v,i}$	System capacitance
$\sum_{i=1}^{N} \left[y_i R_i T \frac{dm}{dt} \right]_S (t)$	Effect on system temperature variation rate of *pv* potential energy variation rate
$\left[(h_{in} - h_S) \frac{dm_{in}}{dt} \right] (t)$	Contribution of enthalpy difference between inlet and system to temperature variation rate
$\left[(h_S - h_{out}) \frac{dm_{out}}{dt} \right] (t)$	Contribution of enthalpy difference between exhaust and system to temperature variation rate
$\dot{Q}$	Effect of heat transfer rate on system temperature variation rate
$\dot{W}$	Effect of work transfer rate on system temperature variation rate

The variation of temperature observed inside an ICE is the result of multiple contributions from energy related terms, Table 1, and can be understood by identifying, adding and measuring the contributions of each term. Figure 6 shows the sources for temperature variation inside an ICE during the combustion stage, its identification and magnitude, both absolute and relative. The *pv* term, for instance, refers to the flow work required to create the Burned Zone (14) and as the figure shows it has by far the biggest contribution to temperature variation. The enthalpy based terms, both h_u and h_b are of similar magnitude but do not vary the same way. Heat transfer is negative, meaning heat is transferred from the ICE to its surroundings and the term related to work was not included. Correlating with **Error! Reference source not found.** it can be noticed that peaks in h_u and pv terms in Figure 6 coincide with peaks in T_u and T_b in **Error! Reference source not found.**. (15) (16)

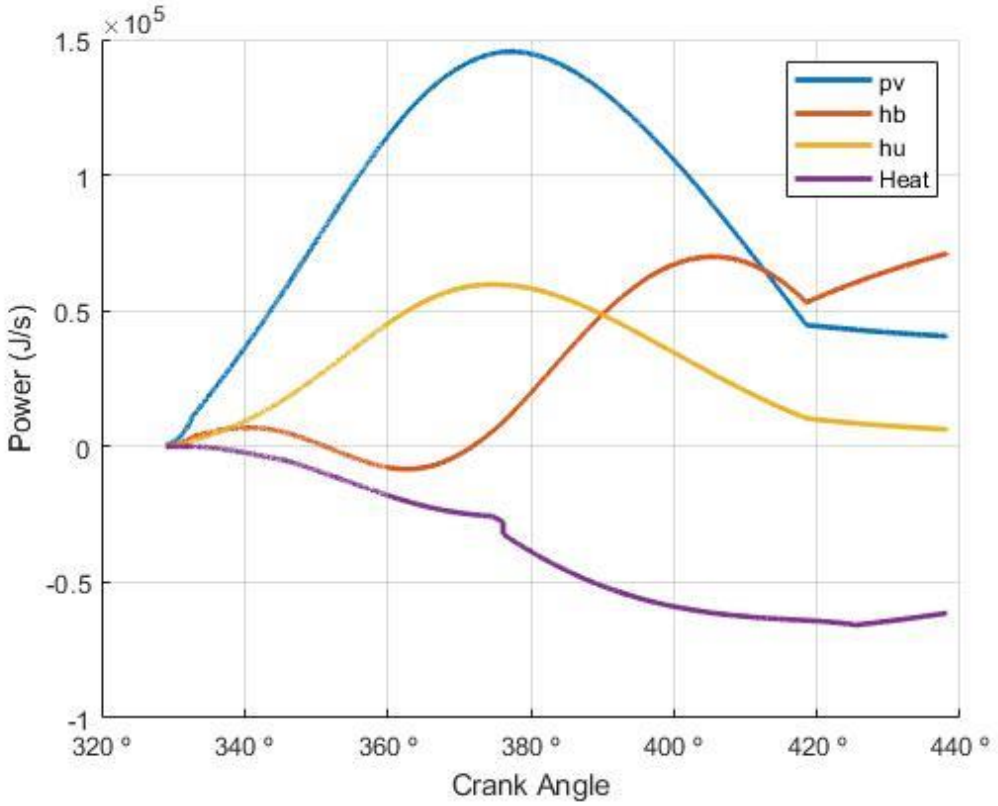

Figure 6: Contributions of the *pv* work flow term, heat transfer, Burned Zone enthalpy and Unburned Zone enthalpy terms to Burned Zone temperature variation rate for 31º ignition timing, 6000 RPM and equivalence ratio of 1.0.

3.7. Equation for mole fraction variation

The initial model was expanded to include the species carbon monoxide, CO; H_2, hydrogen (molecular); H, hydrogen (atomic); O, oxygen (atomic); OH, hydroxide; NO, nitrogen monoxide and N, nitrogen (atomic). The system's composition in Burned Zone was considered variable. This new model assumes instant chemical equilibrium for the reacting system in the Burned Zone at each point in time and means an additional 12 degrees of freedom are introduced. This model is not realistic with regards with an actual ICE but merely a step towards a more realistic depiction of ICE operation. (4) (26)

3.7.1. Chemical equilibrium equations

To model the added degrees of freedom 12 new equations were derived, based on constraints relating to the chemical equilibrium process, atomic species conservation and molar fraction total. The reactions in equilibrium are: (26)

Table 2: Reactions and equilibrium constant equations.

Reaction	Partial Pressure Equilibrium Constant	Equation
$\frac{1}{2}H_2 \Leftrightarrow H$	$K_1 = x_1 \frac{p^{1/2}}{x_4^{1/2}}$	Reaction 1
$\frac{1}{2}O_2 \Leftrightarrow O$	$K_2 = x_2 \frac{p^{1/2}}{x_8^{1/2}}$	Reaction 2
$\frac{1}{2}N_2 \Leftrightarrow N$	$K_3 = x_3 \frac{p^{1/2}}{x_{11}^{1/2}}$	Reaction 3
$\frac{1}{2}H_2 + \frac{1}{2}O_2 \Leftrightarrow OH$	$K_5 = \frac{x_5}{x_4^{1/2} x_8^{1/2}}$	Reaction 4
$\frac{1}{2}O_2 + \frac{1}{2}N_2 \Leftrightarrow NO$	$K_7 = \frac{x_7}{x_8^{1/2} x_{11}^{1/2}}$	Reaction 5
$H_2 + \frac{1}{2}O_2 \Leftrightarrow H_2O$	$K_9 = \frac{x_9}{x_4 x_8^{1/2} p^{1/2}}$	Reaction 6
$CO + \frac{1}{2}O_2 \Leftrightarrow CO_2$	$K_{10} = \frac{x_{10}}{x_6 x_8^{1/2} p^{1/2}}$	Reaction 7

The equilibrium constant for each reaction is defined by the empirical expression:

$$K = 10^{\left[a_{11}\, ln(T) + \frac{a_{12}}{T} + a_{13} + a_{14}T + a_{15}T^2\right]} \quad (3\text{-}20)$$

Where $a_{(i,j)}$ are regression parameters and T is temperature. (26)

3.7.2. Further equilibrium equations

Further equations are derived from the atom balances for the various elements: (26)

Table 3: Conservation of atomic species

C Balance	$x_{\mathrm{CO}} + x_{\mathrm{CO_2}} = n x_{13}$
H Balance	$x_{\mathrm{H}} + 2x_{\mathrm{H_2}} + x_{\mathrm{OH}} + 2x_{\mathrm{H_2O}} = m x_{13}$
O Balance	$x_{\mathrm{O}} + x_{\mathrm{OH}} + x_{\mathrm{CO}} + x_{\mathrm{NO}} + 2x_{\mathrm{O_2}} + x_{\mathrm{H_2O}} + 2x_{\mathrm{CO_2}} = 2r x_{13}$
N Balance	$x_{\mathrm{N}} + x_{\mathrm{NO}} + 2x_{\mathrm{N_2}} = 2r' x_{13}$

Where r, r' and r'' are proportions of N_2, O_2 and Ar in air and x_{13} is defined as the amount of products yielded by one mol of fuel. Furthermore, the constraint that the mole fraction of all the products adds up to unity requires that: (26)

$$\sum_{i=1}^{12} x_i = 1 \tag{3-21}$$

3.8. Expression of mole fraction variation

A symbolic MATLAB program was constructed to derive from the equations in Table 2, Table 3 as well as Eq. (3-21) the equations for the time derivatives of each system component mole fraction for ethanol fuel. The results are shown in Eq. ((3-22) to ((3-33) (31):

$$\frac{dx_{\mathrm{H}}}{dt} = 4\frac{K_1(T)}{p^2T^2} \times \left[p \times T^2 \frac{dx_{\mathrm{H_2}}}{dt} - T^2 x_{\mathrm{H_2}} \frac{dp}{dt} + \ln(10) p x_{\mathrm{H_2}} \frac{dT}{dt} \times (-a_{12} + a_{14}T^2 + 2a_{15}T^3 + a_{11}T) \right] \tag{3-22}$$

$$\frac{dx_{\mathrm{O}}}{dt} = 4\frac{K_2(T)}{p^2T^2}\left[pT^2\frac{dx_{\mathrm{O_2}}}{dt} - T^2x_{\mathrm{O_2}}\frac{dp}{dt} + \ln(10)px_{\mathrm{O_2}}\frac{dT}{dt}(-a_{22} + a_{21}T + a_{24}T^2 + 2a_{25}T^3)\right] \quad (3\text{-}23)$$

$$\frac{dx_{\mathrm{N}}}{dt} = 4\frac{K_3(T)}{p^2T^2} \times \left[p \times T^2\frac{dx_{\mathrm{N_2}}}{dt} - T^2x_{\mathrm{N_2}}\frac{dp}{dt} + \ln(10)\frac{dT}{dt}px_{\mathrm{N_2}}(-a_{32} + a_{31}T + a_{34}T^2 + 2a_{35}T^3)\right] \quad (3\text{-}24)$$

$$\frac{dx_{\mathrm{H_2}}}{dt} = \frac{1}{2} \times \left(\frac{2500}{111} \times \phi \times \frac{dx_{\mathrm{Ar}}}{dt} - \frac{dx_{\mathrm{OH}}}{dt}\right) - \frac{dx_{\mathrm{H_2O}}}{dt} - \frac{1}{2} \times \frac{dx_{\mathrm{H}}}{dt} \quad (3\text{-}25)$$

$$\frac{dx_{\mathrm{OH}}}{dt} = \frac{K_4(T)}{4T^2} \times \left[T^2x_{\mathrm{H_2}}\frac{dx_{\mathrm{O_2}}}{dt} + T^2x_{\mathrm{O_2}}\frac{dx_{\mathrm{H_2}}}{dt} + \ln(10)x_{\mathrm{H_2}}x_{\mathrm{O_2}} \times \frac{dT}{dt} \times (-a_{42} + a_{41}T + a_{44}T^2 + 2a_{45}T^3)\right] \quad (3\text{-}26)$$

$$\frac{dx_{\mathrm{CO}}}{dt} = \frac{5000}{333} \times \phi \times \frac{dx_{\mathrm{Ar}}}{dt} - \frac{dx_{\mathrm{CO_2}}}{dt} \quad (3\text{-}27)$$

$$\frac{dx_{\mathrm{NO}}}{dt} = \frac{K_5(T)}{4T^2} \times \left[T^2x_{\mathrm{O_2}}\frac{dx_{\mathrm{N_2}}}{dt} + T^2x_{\mathrm{N_2}}\frac{dx_{\mathrm{O_2}}}{dt} + \ln(10)x_{\mathrm{O_2}}x_{\mathrm{N_2}}\frac{dT}{dt} \times (-a_{52} + a_{51}T + a_{54}T^2 + 2a_{55}T^3)\right] \quad (3\text{-}28)$$

$$\frac{dx_{O_2}}{dt} = \frac{1250\left(\frac{6}{\phi}+1\right)}{33} \times \frac{dx_{Ar}}{dt} - \frac{1}{2} \times \frac{dx_{OH}}{dt} - \frac{1}{2} \times \frac{dx_{CO}}{dt} - \frac{1}{2} \times \frac{dx_{NO}}{dt} - \frac{1}{2} \times \frac{dx_{H_2O}}{dt} - \frac{dx_{CO_2}}{dt} - \frac{1}{2} \times \frac{dx_{O}}{dt} \quad (3\text{-}29)$$

$$\frac{dx_{H_2O}}{dt} = \frac{K_6(T)}{4T^2} \times \begin{bmatrix} pT^2 x_{H_2} \frac{dx_{O_2}}{dt} + pT^2 x_{O_2} \frac{dx_{H_2}}{dt} + T^2 x_{H_2} x_{O_2} \frac{dp}{dt} + \ln(10) p x_{H_2} x_{O_2} \frac{dT}{dt} \times \\ (-a_{62} + a_{61}T + a_{64}T^2 + 2a_{65}T^3) \end{bmatrix} \quad (3\text{-}30)$$

$$\frac{dx_{CO_2}}{dt} = \frac{K_7(T)}{4 \times T^2} \times \begin{bmatrix} pT^2 x_{CO} \frac{dx_{O_2}}{dt} + pT^2 \times x_{O_2} \times \frac{dx_{CO}}{dt} + T^2 x_{CO} x_{O_2} \frac{dp}{dt} + \\ \ln(10) p x_{CO} x_{O_2} \frac{dT}{dt} \times (-a_{72} + a_{71}T + a_{74}T^2 + 2a_{75}T^3) \end{bmatrix} \quad (3\text{-}31)$$

$$\frac{dx_{N_2}}{dt} = \frac{1}{2} \times \left(\frac{9331}{111} \times \frac{dx_{Ar}}{dt} - \frac{dx_{NO}}{dt}\right) - \frac{1}{2} \times \frac{dx_{N}}{dt} \quad (3\text{-}32)$$

$$\frac{dx_{Ar}}{dt} = -\frac{dx_{H}}{dt} - \frac{dx_{O}}{dt} - \frac{dx_{N}}{dt} - \frac{dx_{H_2}}{dt} - \frac{dx_{OH}}{dt} - \frac{dx_{CO}}{dt} - \frac{dx_{NO}}{dt} - \frac{dx_{O_2}}{dt} - \frac{dx_{H_2O}}{dt} - \frac{dx_{CO_2}}{dt} - \frac{dx_{N_2}}{dt} \quad (3\text{-}33)$$

This subsystem states that the mole fraction variation of each species is the result of the contribution of the variation of the other species as well as temperature and pressure. This contribution is weighted through terms that also depend on mole fraction, temperature and pressure as well as equilibrium constant coefficients. Whereas previously (26) a numerical approach was used to integrate this system of equations, currently, through object oriented programming and symbolic derivation, an exact approach is attempted[3]. (31) (32)

[3] Mole fraction variation was the last part of the model to be derived and, although it has gone through 5 versions it was not implemented computationally with success.

Figure 7 shows profiles of NO, a pollutant and indirect GHG, mass fraction (fraction of total system mass excluding fuel) as function of crank angle and equivalence ratio. The pollutant creation effect of an ICE is clearly visible from Figure 7 as intake air contains no NO but ICE exhaust gases do contain NO and so are pollutant (in the atmosphere acts as an irritant and precursor to the toxic NO_2) and indirectly have a GHG effect. The step occurring at around 360º crank angle is the degree to which ICE pollution is generated. The observed effect is of a step increase in NO levels with combustion, from less than 1 grams of NO per kg of system to 5x that value. The effect of increasing equivalence ratio is to decrease this pollutant emission, which would be explained by there being less oxygen available to oxidize the fuel. Finally, in understanding the pollution effect of ICE operation it should be noted that even though the NO mass fraction is small a normal engine is capable of thousands of cycles per minute. That then has to be scaled with the number of ICE's in operation, which numbers in the millions for Light Duty Vehicles (1). Also of note is that not only NO is released into the atmosphere but also CO_2, CO, hydrocarbons, soot and other pollutants. This will translate into a persistent release of toxic materials into the environment which over time will accumulate and generate effects such as global warming. As pollutants are generated by the ICE's own mode of operation, which can't be changed, this is a challenge for ICE development and, obviously, always a matter to consider when selecting ICE's for energy efficiency. (4) (5)[4]

[4] ICE combustion contains complex chains of reactions and the production of each species occurs through pathways which are not fully understood. The purpose of this calculation is to introduce a deeper level in the operation of an ICE, beyond the bulk production of carbon dioxide and water. (6)

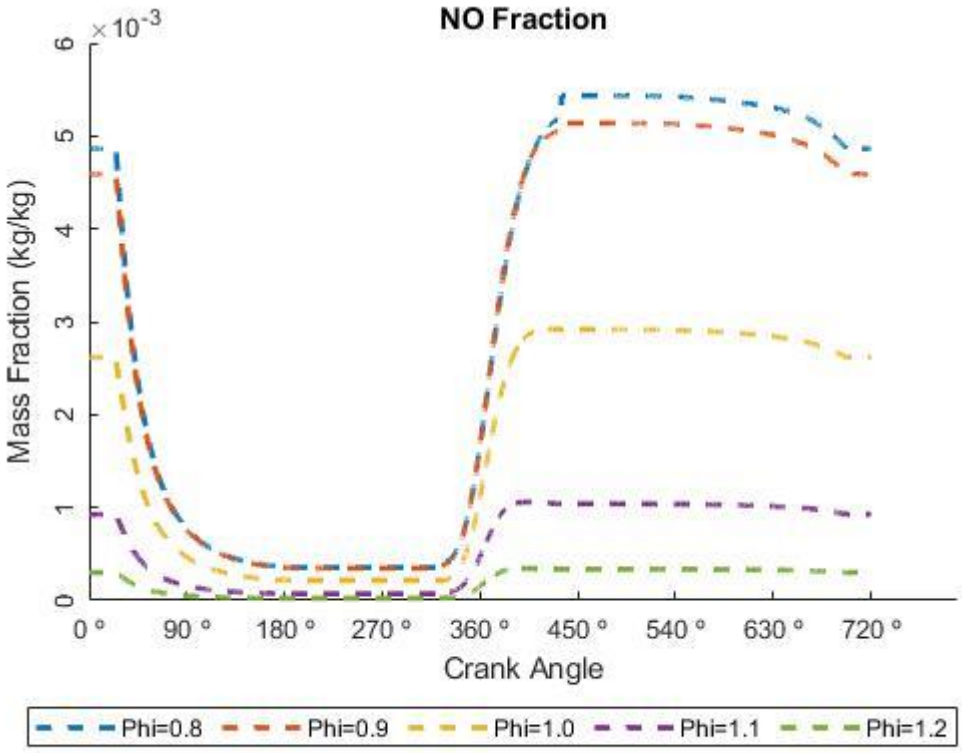

Figure 7: NO mass fraction profiles as function of crank angle for different equivalence ratios

3.9. Equation for additional mass variation

As there is a new source of variation for system component mass, that being the continuous shift in equilibrium, the equation derived in (3-13) requires new terms. The starting principle is that the differential of Burned Zone mass evaluated at time *t* now includes two sources of variation: composition and system amount, Eq. (3-34): (15) (17) (26)

$$d(m_i)_b(t) = [M_i n dx_i]_b(t) + [M_i x_i dn]_b(t) \quad (3\text{-}34)$$

Expanding upon Eq. (3-34), Eq. (3-35) is derived.

$$d(m_i)_b(t) = [M_i n dx_i]_b(t) + \left[\frac{M_i x_i}{M} dm\right]_b(t) - \left[\frac{M_i x_i m}{M^2} dM\right]_b(t) \quad (3\text{-}35)$$

Taking into consideration Eq. (2-2) and correlating for time variation:

$$\left(\frac{dm_i}{dt}\right)_b(t) - \left[M_i \frac{m}{M}\frac{dx_i}{dt}\right]_b(t) + \left[M_i \frac{m}{M^2} x_i \sum_{i=1}^{12} M_i \frac{dx_i}{dt}\right]_b(t) = \left[\frac{x_i M_i}{M} \rho_u S_b A_b\right]_b(t) \quad (3\text{-}36)$$

which yields the new equation for the variation of system mass. It can now be observed that each components' mole fraction in the Burned Zone contributes to the mass variation of one or more of the other Burned Zone components.

3.10. Equation for additional temperature variation

$$[dE]_S(t) = \left[d\left(\sum_{i=1}^{N} y_i e_i\, m\right)\right]_S(t) = \left[m \sum_{i=1}^{N} y_i d(e_i)\right]_S(t) + \left[\sum_{i=1}^{N} y_i e_i\, d(m)\right]_S(t) + \left[m \sum_{i=1}^{N} e_i d(y_i)\right]_S(t) \quad (3\text{-}37)$$

The introduction of a shifting equilibrium condition equally adds a new source for Burned Zone temperature variation, given by the 3rd term in Eq. 3-37. An equilibrium shift is a driving force for temperature variation as the system will evolve from any starting temperature and composition to the corresponding equilibrium composition and temperature. The principle to derive the new terms for equation (3-19) is based on

considering system energy as depending on variable mass fraction for each system component, as seen in Eq.[5] (3-37). (7) (15) (17) (26)

Taking into consideration the notions of molar mass, mass fraction and system energy the following expression for the new term is derived:

$$\left[m\sum_{i=1}^{N} e_i dy_i\right]_S (t) = \left\{\left[\frac{m}{M}\sum_{i=1}^{N} M_i \times [(h_i - h) + (R - R_i)T] \times dx_i\right]\right\}_S (t) \quad (3\text{-}38)$$

3.11. Equations for flame variation

The behaviour of a combustion flame can be explained in two dimensions, its structure, which defines how a flame occupies space, and its speed, which is how fast a flame propagates, propagation which can be in laminar or turbulent regime. Laminar burning regime speed is relevant as it is the base for calculation of turbulent regime speed, the latter being responsible for the peak in energy generation observed in ICE engines. In this work flame speed is modelled in a simplified form, as illustrated in Eq.(3-39): (4) (6):

$$U_b = S_b \times \frac{M_u T_b}{M_b T_u} \times \frac{1 - V_b}{V_u + V_b} + \frac{V_b}{V_u + V_b} \quad (3\text{-}39)$$

Where U_b is mean expansion speed of burning gas, $S_b$is flame speed, M_u and M_b are molar masses of Unburned and Burned Zone, T_u and T_b are the temperature of Unburned and Burned Zone and V_u and V_b are the volume of Unburned and Burned Zone, respectively. (4)

[5] Showing the complete derivation of these equations is not feasible so merely its start, end and main principles are shown.

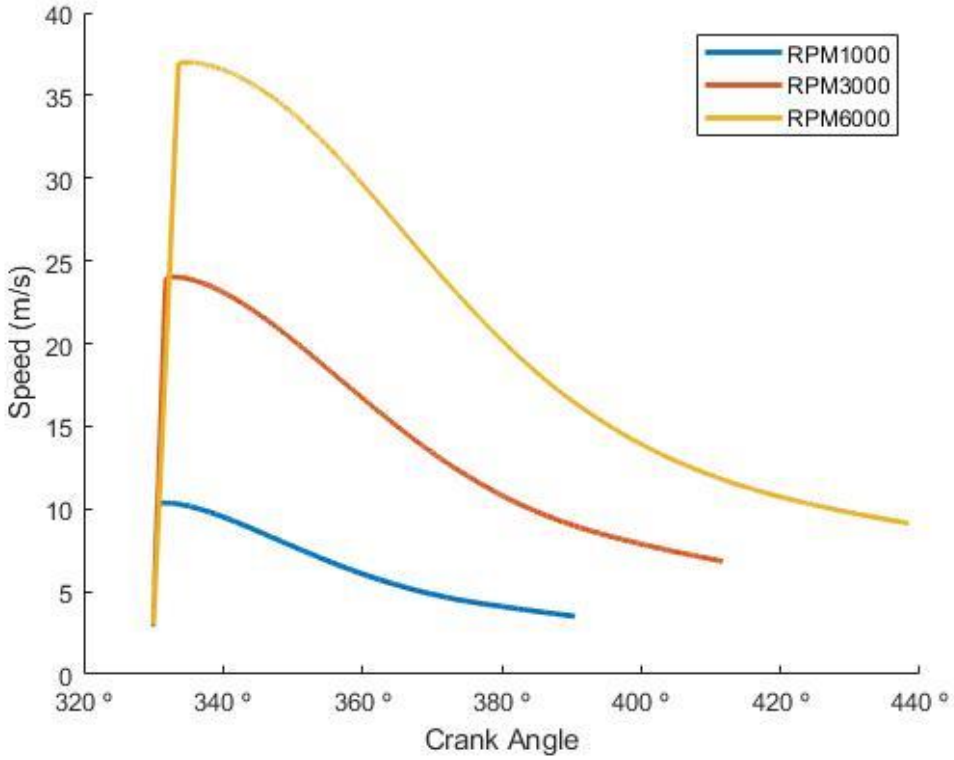

Figure 8: Mean expansion speed of burning gas as a function of crank angle for several engine rotational speeds

Figure 8 shows mean expansion speed of burning gas as a function of crank angle over several engine RPM, at 30º ignition timing and for an equivalence ratio of 1.0, during an ICE's combustion stage. It can be observed that there is a visible effect of engine RPM on mean expansion speed of burning gas. One effect is that increasing engine RPM causes combustion to last longer, a 60º increase from 1000 RPM to 6000 RPM. Another effect is peak speed also increases with engine RPM: mean expansion speed of burning gas is 3.5× higher for 6000 RPM compared to 1000 RPM. (16)

3.11.1. **Equation for Kolmogorov scale variation**

The Kolmogorov length scale is a measure of flame structure and is a factor in determining flame turbulence, turbulence being key in the rate of fuel consumption. Figure 9 displays the effect of engine rotational speed on turbulence, as expressed by Kolmogorov

length scale. The lower the Kolmogorov length scale the higher the turbulence, so it is observed that maximum turbulence occurs at around 370º crank angle, which follows ignition timing. The effect of increasing engine rotational speed is to decrease Kolmogorov length scale and promote turbulence, enabling a higher rate of energy conversion. (4)

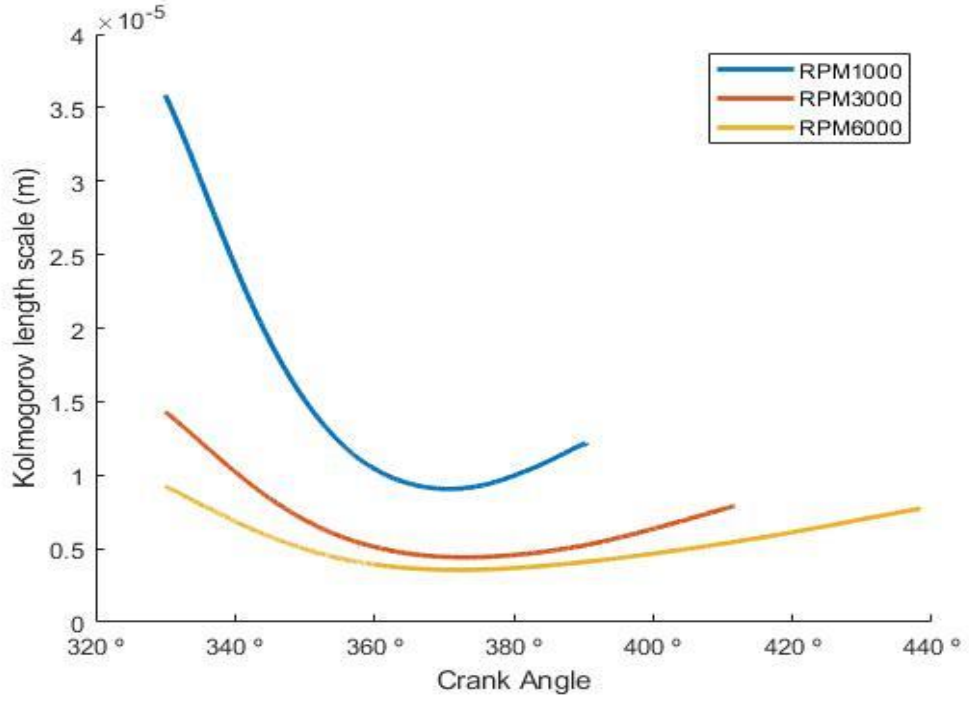

Figure 9: Effect of engine rotational speed on Kolmogorov length scale

3.10 Equation for Knock Variation

$$\tau = \frac{17.68}{1000} \times \left(\frac{\mathrm{ON}}{100}\right)^{3.402} \times \left(\frac{p}{101325}\right)^{-1.7} \times e^{\frac{3800}{T_u}} \qquad (3\text{-}40)$$

The τ parameter is termed ignition delay and is related to Knock occurrence, Knock being the phenomena of abnormal combustion which can halt ICE operation and even damage it. The lower the value of τ the greater the probability of occurrence of Knock. As can be seen from Eq. (3-40), τ is a function of ON (octane number, a parameter specific to each fuel, characterizing its resistance to Knock occurrence), pressure and temperature (of Unburned Zone). τ grows with ON but is inversely proportional to temperature and pressure.

(4) (29) As can be seen in Figure 10 the effect of increasing engine RPM on τ is not significant with the spacing between curves being minimal. (4)

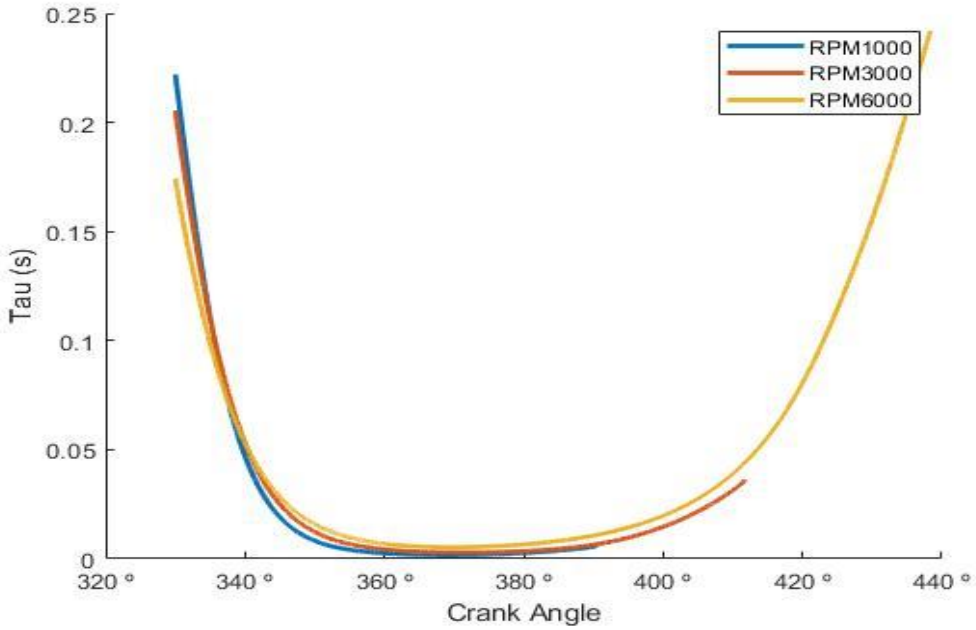

Figure 10: Effect of engine rotational speed on τ at 30º BTDC ignition timing and 1.0 equivalence ratio during Combustion Stage.

3.12. Heat transfer

To calculate engine heat transfer a modified Annand heat transfer model was used and to calculate heat transfer areas the "Autodesk Inventor" 3D modelling software was used with a 3D model of the engine combustion chamber. "Autodesk Inventor" enables the estimation of combustion chamber areas available for heat transfer both for Unburned and Burned Zone as the flame progresses. (4)

$$h_{conv} = k_u \frac{a_{annand}}{B} \times \left(2 \times \rho_u \left|v_{(g,u)}\right| \times B/\mu\right)^{b_{annand}} \qquad (3\text{-}41)$$

In Eq. (3-41) h_{conv} is the convective heat transfer coefficient, B is cylinder bore, k_u is unburned gas thermal conductivity, ρ_u is unburned gas density, $v_{(g,u)}$is unburned gas velocity and μ is unburned gas dynamic viscosity. a_{annand} and b_{annand} are parameters

specific to the Annand heat transfer model. Eq. (3-41) illustrates a key parameter in heat transfer, the coefficient for heat transfer through convection. In an ICE three types of heat transfer occur: radiation, conduction, and convection. In ICE's the convection process is dominant as expressed by h_{conv}. (4)

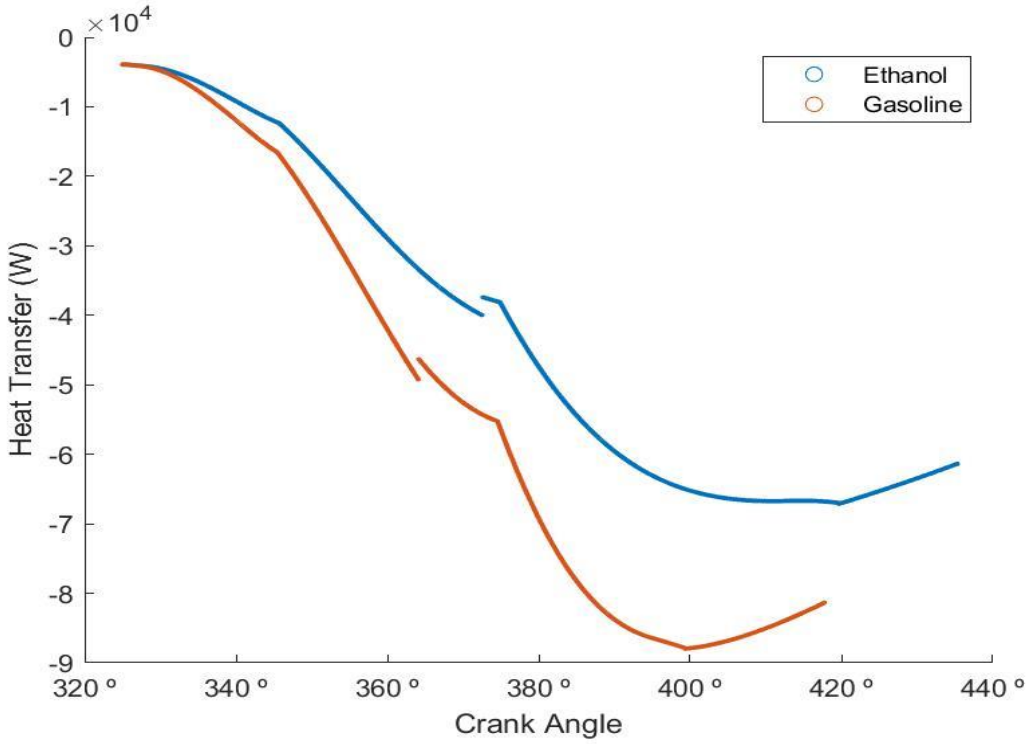

Figure 11: Heat Transfer rate of gasoline and ethanol, measured at 6000 RPM, equivalence ratio 1.0 and ignition timing 35°.

Figure 11 shows the comparison of heat transfer between and ethanol fuelled ICE and gasoline fuelled one. It is observed that ethanol combustion transfers heat at a lower rate than gasoline, the cause being that despite a lower thermal conductivity of gasoline combustion products the gasoline combustion system reaches higher temperatures.[6] **(4) (11)**

[6] The discontinuity observed in Figure 11 is due to an imperfection in the regression model.

4. MODEL RESOLUTION

The model developed in sections 2 and 3 is a collection of five systems of ODE's (section 4.2), one for each stage, which are solved as a whole through an iterative scheme (section 4.1) and implemented computationally (section 5). Solving such a problem requires consideration of: (24) (33) (34) (35)

- **readability**: model and its resolution should be simple;
- **complexity**: the model should explain the most variation possible;
- **speed**: the solution should be quick and efficient;
- **accuracy**: the solution encountered should be accurate;
- **cost**: the computational cost in solving the model should be minimized.

The iterative scheme selected simulates an engine cycle, where the initial conditions for one stage are the conditions at the end of a previous stage. (30) (34) (35)

4.1. Iterative scheme

The mole fraction of residual burned gases is the parameter being iterated. After being initialized, based on a reasonable estimate it is iterated at the end of each cycle, as a result of the engine's own operation in the following manner:

$$m_{rbg} = m_{in,c}(sB) + m_S(TDC) + m_{exh}(sA) \quad (4\text{-}1)$$

The meaning of the variables is:

m_{rbg}: residual burned gases mass;

$m_{in,c}$: contribution from intake manifold to residual burned gases, measured at the end of crossflowBTDC stage;

m_S(TDC): contribution from system mass at Top Dead Centre to residual burned gases, measured at the end of crossflowBTDC stage;

$m_{exh}(sA)$: contribution from exhaust to residual burned gases, from the flow from exhaust manifold to the system between the end of crossflowBTDC stage and the end of crossflowATDC stage.

The criteria used for convergence is the difference between the temperature obtained at the end of the Intake Compression stage in consecutive iterative cycles. When the temperatures of two consecutive cycles are under a specified tolerance convergence is assumed. (35) (36)

4.2. Mathematical model

Mathematically, each stages' model takes the form of a system of ODE's as $A(t,y) \times \dot{y} = f(t,y)$, which translates to: (13) (24) (30) (37)

$$\begin{bmatrix} g_{1,n}(t,y) & \cdots & g_n(t,y) \\ \vdots & \ddots & \vdots \\ g_{n,1}(t,y) & \cdots & g_{n,n}(t,y) \end{bmatrix} \times \begin{bmatrix} \frac{dy_1}{dt} \\ \vdots \\ \frac{dy_n}{dt} \end{bmatrix}(t) = \begin{bmatrix} f_1(t,y) \\ \vdots \\ f_n(t,y) \end{bmatrix} \quad (4\text{-}2)$$

Here *A* is termed a "mass matrix" which in this model's case is dependent upon time (not constant) and on the systems' state (state dependent). *A* contains all the terms that directly influence system variation, which is expressed by the vector including all the time derivatives of system state variables. The second member of the ODE system, the *f* vector, is equally state dependent and expresses each value of each state variable variation. (34), (37). Various models were constructed during this work, which meant the dimensions of *A* grew from an initial dimension of 6 to a final of 45. It is also of note that this ODE system varies from stage to stage, e.g. a 45-dimension model was used in Combustion Stage and a 17-dimension model for Intake Compression stage. (34)

5. MODEL COMPUTATION

This model was implemented computationally through MATLAB (Matrix Laboratory), version R2019b, licensed by the University of Coimbra. (37) The following is an overview of the computation principles followed in designing the computer program which implements the theoretical model. (13) (23) (24) (38) (39) (40)

5.1. Computational principles

5.1.1. Programming unit design

```
[yCO2b,yH2Ob,yN2b,yO2b,yCOb,yH2b,yHb,yOb,yOHb,yNOb,yArb]=

deal(... % kg/kg

y(30)*MM.CO2/Mb,y(31)*MM.H2O/Mb,y(32)*MM.N2/Mb,y(33)*MM.O
2/Mb,... %kg/kg

y(34)*MM.CO/Mb,y(35)*MM.H2/Mb, y(36)*MM.H/Mb,

y(37)*MM.O/Mb,... %kg/kg

y(38)*MM.OH/Mb,y(39)*MM.NO/Mb,

y(40)*MM.Ar/Mb,y(41)*MM.N/Mb); %kg/kg

% fração mássica de CO2,H2O,N2,O2,CO,H2,H,O,OH,NO e Ar

% nos gases residuais, (kg de espécie/kg zona Não
Queimados),

update 7

% mol de espécie^(1-1)*mol de gases residuais^(-1+1)*

% kg de espécie^(1)*kg de gases residuais^(-1)*
```

As shown above (an excerpt of the MATLAB program for the Combustion Stage). MATLAB programs are constituted by diverse units, each having its own function, integrated as building blocks of the program as a hole. In the example above the unit is a

piece of code arranged as a block, which assigns the value of a vector (the *y* vector) through the MATLAB "deal" operation. Each programming unit receives, produces, stores and transmits data to other programming units. One key feature when designing such units is ensuring data quality. For that purpose, ideally, each unit should have a control centre, capable of filtering data to ensure data quality. During this work that structure was not created so data entry, exit, production, and storage was labelled but not checked, as showcased in the green section of the programming unit above, in Portuguese. One key feature of programming units is that they can undergo different stages of development (the update concept described in section 5.1.4 and they can be interconnected with other programming units. So there is a point beyond which it is not advisable to try and recreate them, but merely to copy them (which would lead to replication errors, equally outside the scope of this work). (24) (32) (41)

5.1.2. Symmetry

When dealing with vectors in MATLAB, checking for symmetry is an essential technique as for large vector (over 1,000 elements) manual verification is unfeasible. Shown below is the illustration of the symmetry between two vectors included the comb.m program developed in this work:

```
R.CO2,R.H2O,R.N2,R.O2,R.CO,R.H2,R.H, R.O,R.OH, R.NO, R.Ar

R.CO2,R.H2O,R.N2,R.O2,R.CO,R.H2,R.H, R.O,R.OH, R.NO, R.Ar
```

In this case the two vectors match and are deemed equivalent. (24) (39)

5.1.3. Program organization

The MATLAB program developed is quite large (over 10,000 lines in total) so much so program access would be infeasible without proper organization. The organization selected includes partitioning the MATLAB program onto levels: cycles, program components and sections:

Greek letters: Alpha, Beta, etc... denote iterative scheme related cycles and measurement protocols.

Roman letters: denote program components, such as the main program (part A) and functions comprised in each program (indexed as B, C, D, ...)

Numbers: To organize each program part numbers are used, starting with roman numerals, I, II, III, ... to denote program sections and Arabic numerals (1,1.1 up to 1.1.1) to denote either relevant statements of each section or subsections.

A cycle, such as an iterative or measurement cycle, represents the top hierarchical structure of the program. Program components are parts of a program (e.g. functions) which can operate by themselves but require data inputs and are able to provide data outputs. Program components are somewhat autonomous but connected. Finally, sections are the different levels of a program component. Sections can't exist by themselves but are interconnected with other sections of the same program component. (24) (37)

5.1.4. Programming methodology

An essential feature in constructing the computer program is the notion of "update"[7], which is illustrated in its three dimensions as followed. This method was devised by the author of this thesis and it is this author's responsibility, even if it was the product of a review of available computer programming techniques: (38) (39)

Horizontal update: to model a process a variable is first initialized (update H level 0). Once that variable is assigned to other variables (thus forming a chain), the update grows by 1 unit. This way, if a program variable reaches update level H17 this means 17 steps were required to evaluate it.

Vertical update: often expressions, code blocks or even programs can be improved or upgraded. This constitutes a vertical update, meaning a new version is available. This update was labelled "Vertical" and termed Update V1, V2, ... This means that if an expression or a function have Update Level V10 then this means 10 previous versions of this expression

[7] The notion of "update" was created by the author of this thesis, Pedro Gonçalves, synthesizing the multiple diverse notions regarding computer program elaboration.

existed. Different versions of the same program will have benefits and drawbacks in relation to each other.

Longitudinal update: this refers to updating within a cycle, for instance when measuring a program variable it can be decided to what extent it will be perceived. Maybe only its final value, maybe its entire value stream should be looked upon or, in a more in-depth approach, looking at its indirect effects on other variables. This way if an expression has Update Level L5, this means 5 iterations were required to reach the measurement of such a value.[8]

Table 4: Programming Methodology

$Y=a_{1;}$	Initialization (Horizontal update = H0)
X=Y;	First assignment (Horizontal update = H1)
Z=X;	Second Assignment (Horizontal update = H2)

5.1.5. Solver selection

The solver selected was MATLAB's ODE45, which is the most basic solver in MATLAB. ODE45 is based on the Runge-Kutta method, an iterative numerical method for solving systems of ordinary differential equations, in the case of ODE45 a Runge Kutta method of 4^{th}-5^{th} order. The main issue with more sophisticated solvers was the lack of a Jacobian matrix, the difficulty in computing approximations for first derivatives and the sheer complexity of the model being computed. The SIMULINK tool set perhaps contains solvers more efficient than the ODE45 used here but the SIMULINK environment proved beyond the scope of this work. Still, solution run times ranged from 0.5 seconds to 60 seconds, which constitutes and acceptable timeframe. The key parameters in affecting solver performance were model complexity and conditioning. An increase in model dimension from 30-dimension to 45-dimension means an iteration time 4x larger. The ill conditioning

[8] The notion of "longitudinal update" was used but not developed during this work.

of the model[9] being used means numerical instability and was one of the reasons only ODE45 was tried. (34) (37)

5.2. Error sources

To have an effective computer model error sources must be identified. The following points are a brief list of all error sources discovered during the creation of the computer program, their definition, meaning and how they were tackled (and also if they were resolved or not). (23) (24) (37) (39)

5.2.1. Transcription and coding errors

Transcription errors start by being harmless when coding starts and is performed manually. They become more and more intractable as the model program grows. Transcription errors are also exceedingly difficult to detect as they tend to be random. During this work it was the most common source of error. A transcription error is defined as an error that arises when transcribing a formula or idea on to code, i.e: (13) (24) (30)

Original=$[u_1,u_2,u_3,u_4,u_5,u_6,u_7]$ → Transcribed=$[u_1,\mathbf{v_2},u_3,u_4,u_5,u_6,u_7]$

Example of Transcription Error

MATLAB implies its own syntax and grammar, which follow rules and norms. The challenge during this work was to understand code properly, more than learning how to use it. The biggest challenge in MATLAB coding were the options which come in using a particular MATLAB command. (39)

5.2.2. Modelling error

During system design (section 2) errors can be committed. Those errors can then pass on to implementation stage and create computational errors which at a first approach will not be detectable. Key here is to have the patience to track back and review the model

[9] The model being ill conditioned, particularly during combustion stage, means a solution can be found for 8000 RPM but not 7999 RPM, in what seems an arbitrary process.

itself, if needed. The added benefit is that creating a computer program can serve as an improvement to a model. (30) (37) (42)

5.2.3. Data related errors

All computer programs are based on data. Data generation, transmission, storage and reception are the essential operations of any program unit. The consequence is that data related errors are virtually inevitable, which can affect program stability if they are not controlled. Considering the program developed here has over 10,000 lines and that it is constituted of numerous communicating units, data flow is constant and in practice impossible to fully track. The cause for any abnormal system behaviour is caused by conflicting data signals being emitted by one or more sources.

The recommended way to mitigate data related errors is through creating data structures and attributing patterns to them. Once a structure is defined in an unique pattern it can be identified, modified, worked on and transmitted, making any error it contains less damaging or likely to propagate. (24) (25) (37)

5.2.4. Convergence errors

Convergence errors are errors that occur during the iterative process of the models' resolution. The model designed was ill posed: at the start of the Burned Zone its mass is zero, which mathematically translates to the mass matrix of the ODE system as defined in section 4.2 containing a singularity. This singularity means the problem cannot be solved by ordinary ODE solvers such as ODE45 but is in essence a DAE problem (algebraic differential equations), a mix of differential and algebraic equations. Solving DAE problems proved beyond the scope of this thesis. The way to overcome this issue was to create the *fmass* parameter, which assumes a fictitious initial mass for the Burned Zone. Even with this parameter the mass matrix's condition number was usually around 10^-15 (a number closer to 1 is ideal) and using such a technique created defects in the profiles obtained, observable in the bump of the pressure-volume diagram of section 6.1). Another way to stabilize this problem was to install a specific MATLAB routine to identify when the system was ill posed and so allow recognition of problematic areas. (25) (43)

5.2.5. Dimensions/Units related errors

A simple way to check for errors in code block variables which have physical value through dimensional analysis, particularly if the blocks are of a large dimension. Use of incorrect units is also a source of error, for instance some data sources read temperature in R whereas temperature is read in other data sources in K. (13) (38) (40)

5.2.6. Connection errors

Connection errors present the most challenge error source. As the number and type of program code blocks grew so did the connection between them, exponentially so. This makes connection tracking a particularly challenging issue. The solution is to construct adequate index functions, which will store and transmit information on all connections but at the end of this work that was not fully achieved. (23) (37) (42)

5.2.7. Error propagation and tracking

Error is capable of multiplication and propagation. One error source can give way to a whole chain of simultaneous errors. The solution to this problem is through error tracking routines which detect an error the first time it appears and can track down its origin. Multiple error sources were not fully understood during this work. (24) (38)

5.2.8. Detrimental effects

The conclusion of this section is that, firstly, all errors contribute to affect in a detrimental way a solution. That contribution can vary in magnitude and relevance and in real large programs such as the one developed here not all error sources can be detected or eliminated fully. In fact, there is an uncertainty associated to the error process. The solution here encountered is to develop embedded program structures to minimize and control those error sources, so the solution is stable. (44)

6. RESULTS

6.1. Pressure-Volume diagram

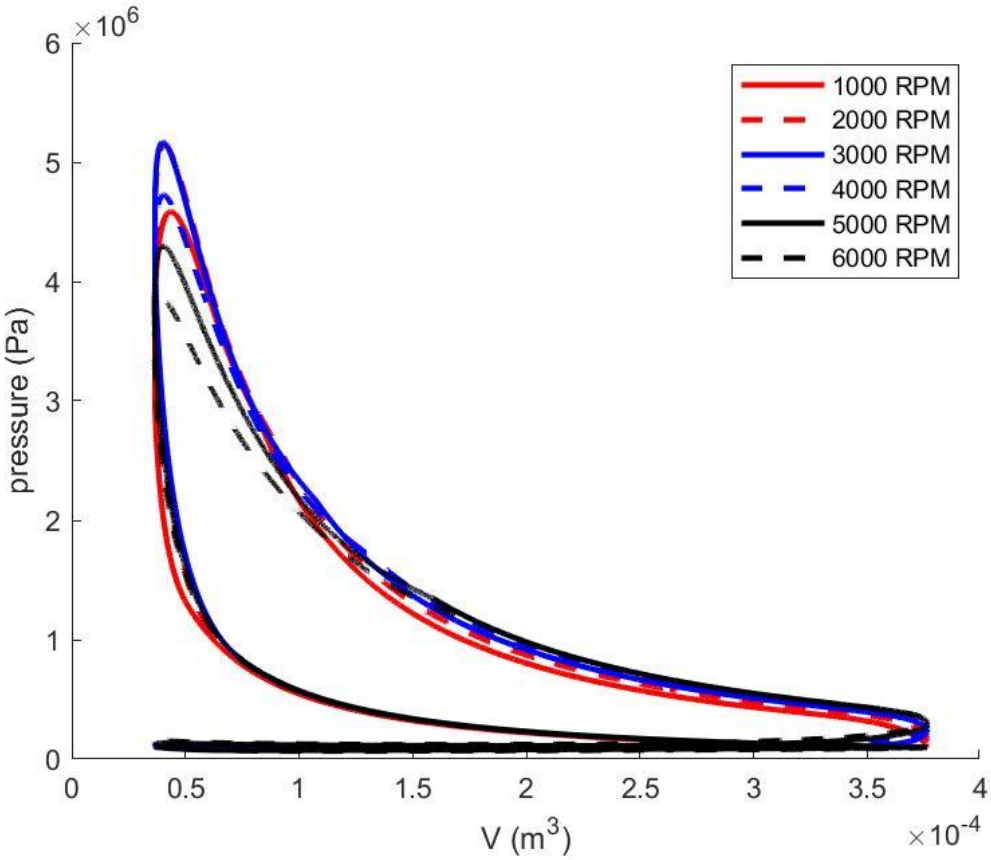

Figure 12: Pressure-volume diagram as a function of engine rotational speed at maximum indicated torque ignition timing and 1.0 equivalence ratio with ethanol as fuel.[10]

The relationship between pressure and volume is key to understand ICE operation as the pressure-volume correlation gives the amount of work the engine can produce. The shape of the pressure-volume diagram is the one predicted for the Otto cycle and, as can be seen by Figure 12, there are two regions in this graph: the top area in between pressure-volume curves corresponds to work produced by the engine and the bottom one,

[10] All graphs shown in this section were built using the MATLAB program developed.

smaller (here negligible) area between pressure-volume curves expresses mechanical work lost due to pumping working fluid through the intake and exhaust ports (11). Being more specific, the range of variation for pressure and volume is from 0.5 bar to 58 bar (10x increase) and from 36 to 376 cm^3 respectively, volume variation in agreement with the engine's compression ratio.

For a given RPM if ignition is timed too late the pressure peak achieved in the engine will be lower and the work transferred onto the piston from the engine gases will also be lower. If ignition is timed too early less work is transferred from the engine gases onto the piston as before TDC more work is transferred from the piston onto the engine gases, which constitutes a loss of available work. The consequence of these two effects is that outside optimal ignition timing work transfer is not maximal. Considering that each RPM curve is constructed at optimal ignition timing it is observed that the optimal engine rotational speed is 3000 RPM, due to the area of the top region in the pressure-volume diagram being larger at 3000 RPM than at any other engine rotational speed (the pressure peak reached at 3000 RPM is superior to peaks at other RPM and at any other point in the pressure-volume curve the 3000 RPM pressure is not inferior to pressure at other RPM). (4) (11) (30)

6.2. Temperature profile

Temperature inside an ICE can reach very high values, in this case over 2500 K. **Error! Reference source not found.** displays the temperature profiles in the Burned Zone and Unburned Zone of an ICE during its combustion stage. The Unburned Zone starts at the start of the engine cycle and ends when the fuel has been consumed. The Burned Zone, on the other hand, starts at ignition timing and ends at Top Dead Centre at the end of the crossflowBTDC stage. Both zones' temperature profiles are distinct, the Burned Zone being obviously higher in relation to the Unburned Zone. In fact, there is a 1500 K step gain during ignition from the Unburned Zone temperature to the Burned Zone temperature. Peaks for both zones' temperature occur a while after ignition timing and the observable effect of engine rotational speed is mixed: on one hand higher engine rotational speeds correlate to

lower temperature peaks in both Unburned and Burned Zone. On the other hand increasing engine rotational speed increases temperature at the start and end of the cycle. (4) (11) (30)

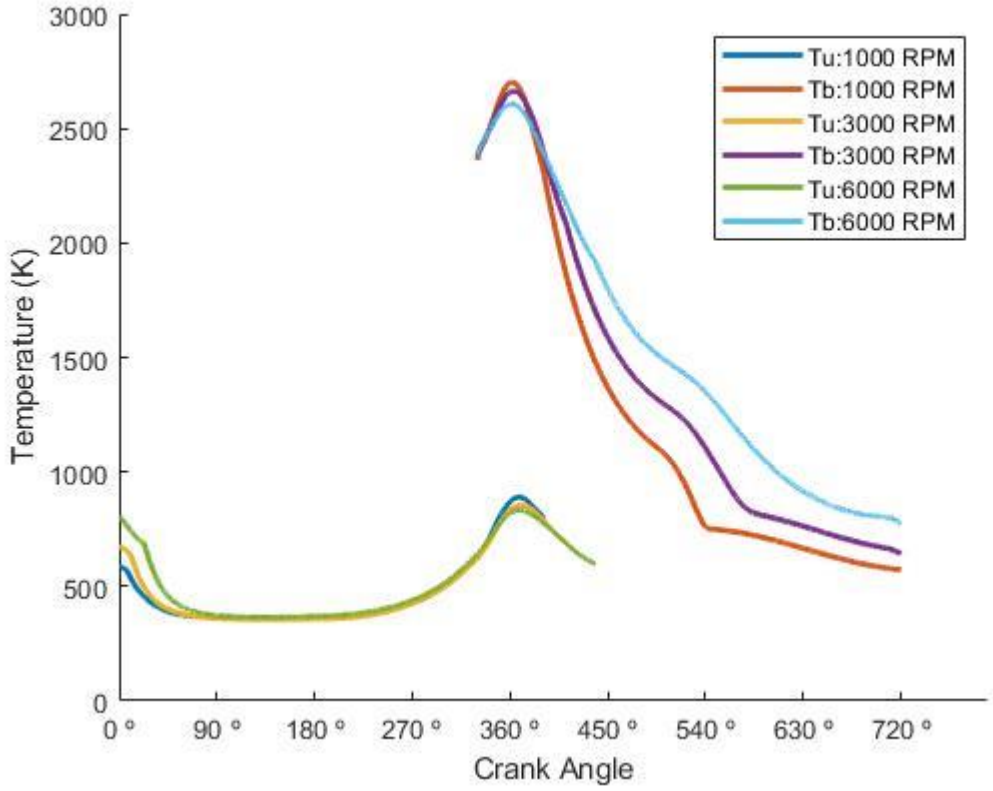

Figure 13: Temperature profiles in Unburned and Burned Zone for engine rotational speeds of 1000, 3000 and 6000 RPM. Ignition timing 30º BTDC, equivalence ratio 1.0.

6.3. Mass profiles

Inside an ICE mass profiles for each of the engine combustion system components exist and evolve over time or crank angle. The evolution matches the conversion of unburned onto burned species as well as the effect of intake and exhaust valves. Burned residual gases persist from cycle to cycle albeit at varying amounts (it is of note that variation between engine cycles should be minimized). In order to observe mass profiles of each species involved in ICE operation (as defined in section 3.7.1) Figure 14 was constructed. Figure 14 displays the mass profiles for each Engine Combustion System species as a

function of crank angle. From Figure 14 it is clearly observed there are two tiers in terms of component mass. The more abundant species, CO_2, H_2O, N_2, O_2, and Argon and the least abundant species, CO, H_2, H, O, OH and NO. It can also be observed that O_2 is essentially converted onto CO_2 and H_2O, CO_2 being GHG inducing. The conversion of reactants onto products is also clearly visible: from 0º to 360º fresh mixture related species dominate; post ignition, from 360º to 720º, combustion products dominate. This highlights the ICE effect of converting valuable resources such as fuel onto GHG gases, an ever-present environmental cost. The second observation is that a side effect of ICE operation is to convert inert gases, not useful for propulsion, such as nitrogen, onto toxic gases such as nitrogen oxides. (4) (30)

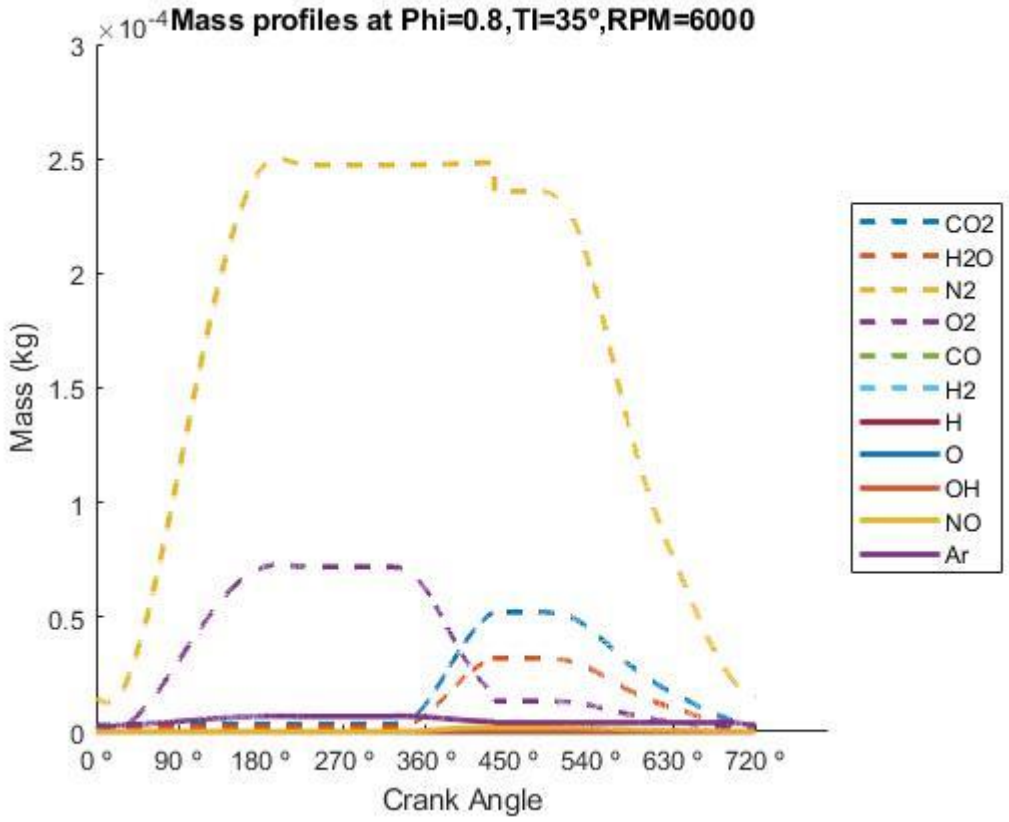

Figure 14: Mass profiles for Engine Combustion System species over crank angle, equivalence ratio 0.8, ignition timing 35º, 6000 RPM.

6.4. Torque profile

Engine Torque is related to the ability of an engine to produce rotational energy. An ICE's rotational energy is important as it can be transmitted to a power shaft or an electricity generator. Figure 15 shows the Torque the ICE can produce under the specifications given in section 2 for ignition timing range of 5° to 45° and engine rotational speed from 1000 to 8000 RPM. The first observation is that the predicted range for Torque is from 37 to 105 N·m, that is a 65% variation. Secondly, it is observed that Torque depends on ignition timing and engine rotational speed, as evidenced by the surface not being flat. The surface graph is in fact concave, reaching an optimum operation point of 105 N·m at 35º ignition timing and 3000 RPM. Correlating Torque variation with ignition timing and engine rotational speed, it is observed that for a fixed ignition timing the loss in Torque with increasing RPM is around 10% per 1000 RPM increase. If RPM is fixed the gain in Torque with increasing TI is around 2.5% per 5° increase. This would imply that in the case of this engine, rotational speed has a higher effect in Torque than ignition timing. (4) (30)

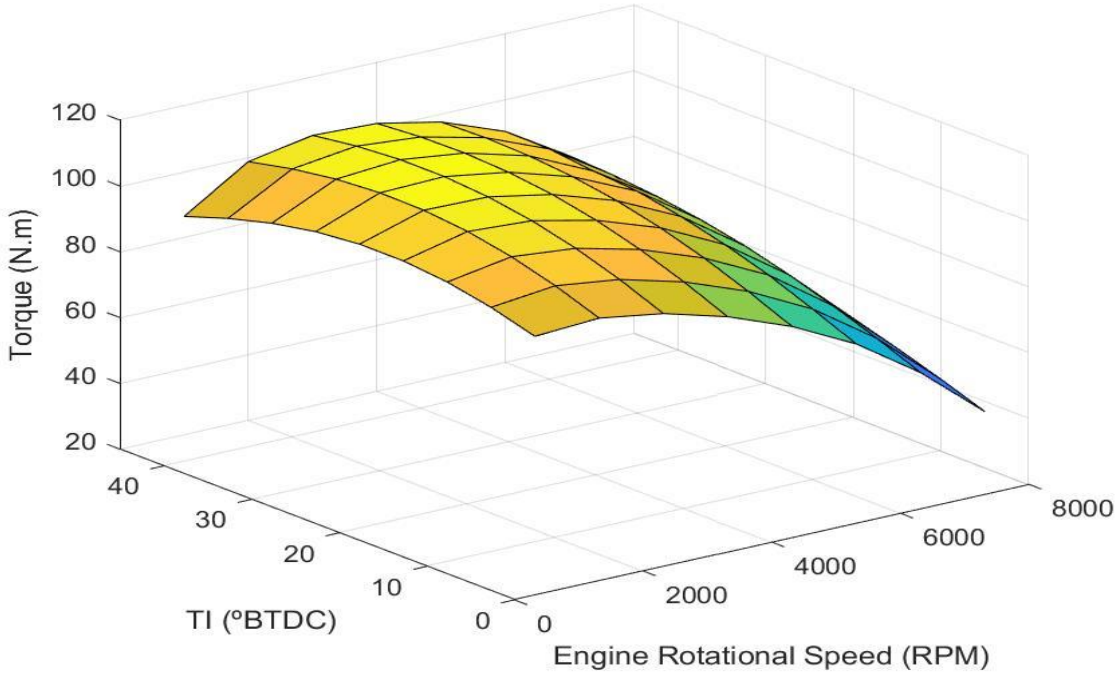

Figure 15: Engine Torque as a function of ignition timing (TI) and engine rotational speed (RPM) at equivalence ratio 1.0.

6.5. Specific fuel consumption profile

Specific fuel consumption is relevant as it measures the conversion of fuel onto ICE power. The higher the specific fuel consumption the least fuel efficient the ICE is. Figure 16 shows specific fuel consumption as a function of ignition timing (degrees BTDC) and engine speed (RPM). Specific fuel consumption depends on both ignition timing and engine rotational speed. That relationship is shown in the form of the curved surface presented in Figure 16. The surface graph is convex, meaning there is an optimal operating point at 30º BTDC and 2000 RPM of 382.6 g/kWh. It is observed that for a fixed ignition timing increasing RPM leads to an on average 10% increase in specific fuel consumption per 1000 RPM. For a fixed engine rotational speed an increase in ignition timing leads to a 2% on average decrease in specific fuel consumption per 5° increase in ignition timing. The conclusion is that engine rotational speed has a greater effect in specific fuel consumption than ignition timing. (4) (30)

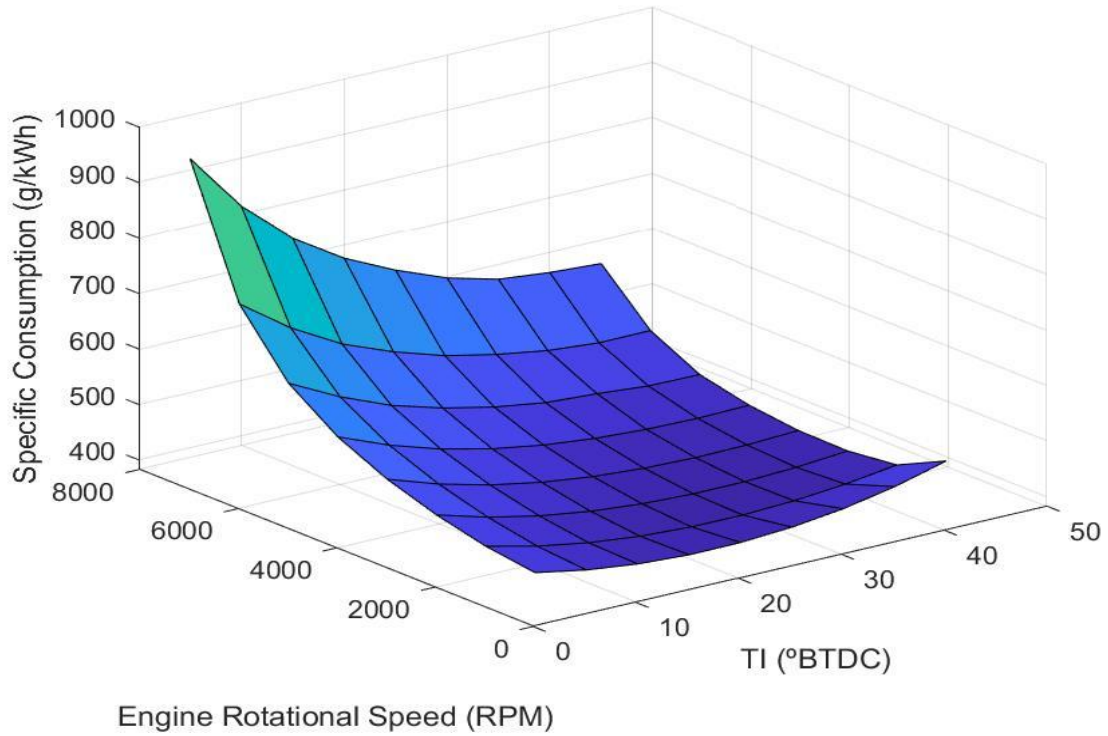

Figure 16: Specific fuel consumption as function of ignition timing (TI) and engine rotational speed (RPM) at equivalence ratio 1.0.

6.6. Power profile

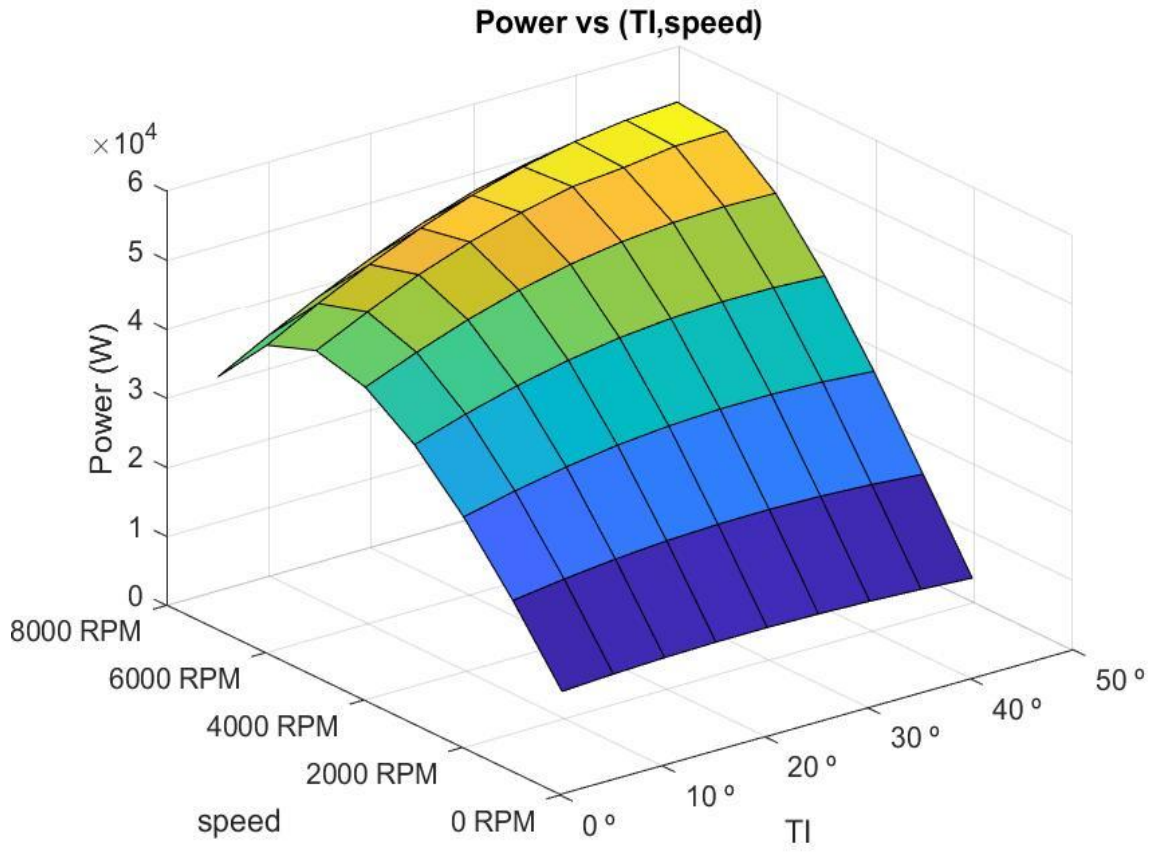

Figure 17: Power as function of ignition timing (TI) and engine rotational speed (RPM) at equivalence ratio 1.0.

ICE's are machines capable of producing and transmitting power through the straightforward mechanism seen in section 2, e.g. for transportation. As can be seen in Figure 17 the ICE with the particular specifications of section 2.1 produces power between 10 and 57 kW and its power production is correlated to two parameters: engine rotational speed and ignition timing. The graph obtained is concave: in general increasing rotational speed and ignition timing leads to increase in power produced up to reaching an optimal of 57 kW at ignition timing of 45º BTDC and at engine rotational speed of 7000 RPM. Minimum power production occurs at 1000 RPM and 45º BTDC ignition timing and, as with Torque, for each

engine rotational speed there is an ignition timing that corresponds to optimal power production. (4) (11) (30)

6.7. Ethanol and gasoline energy efficiency

The power output of an ICE depends on fuel chosen, some fuels will deliver more power output than others, based on their chemical composition and properties. Fuel conversion efficiency is the efficiency of conversion of the chemical energy of the fuel into mechanical energy. Fuel conversion efficiency is just as relevant as power when selecting an ICE: power is correlated to engine size whereas fuel conversion efficiency is to be maximized. Figure 18 displays the comparison between ethanol and gasoline as fuels as far as power production and fuel conversion efficiency are concerned over a range of engine rotational speeds (RPM).

One conclusion is that gasoline and ethanol share similar trends when it comes to power production and conversion efficiency, for instance ethanol reaches reaches peak fuel conversion efficiency at 2000 RPM and gasoline at 3000 RPM. Another conclusion is that, as can be seen from the graph, a gasoline fuelled ICE always produces more power than an ethanol fuelled ICE, regardless of operating engine speed. This helps explain the advantage of gasoline over ethanol, despite gasoline contributing more to GHG emissions. Furthermore, gasoline also has a higher fuel conversion efficiency than ethanol, regardless of engine RPM. So in these two critical energy efficiency parameters gasoline is superior to ethanol, again explaining the wider diffusion of gasoline ICEs in comparison with ethanol fuelled ICEs.

It is of note, that ethanol has a higher octane number than gasoline and so can operate at higher compression ratios, which is a benefit compared to gasoline both in power production and fuel conversion efficiency. Another benefit of ethanol is its cleaner burn as compared to gasoline as well as ethanol being a renewable fuel. (1) (4) (30)

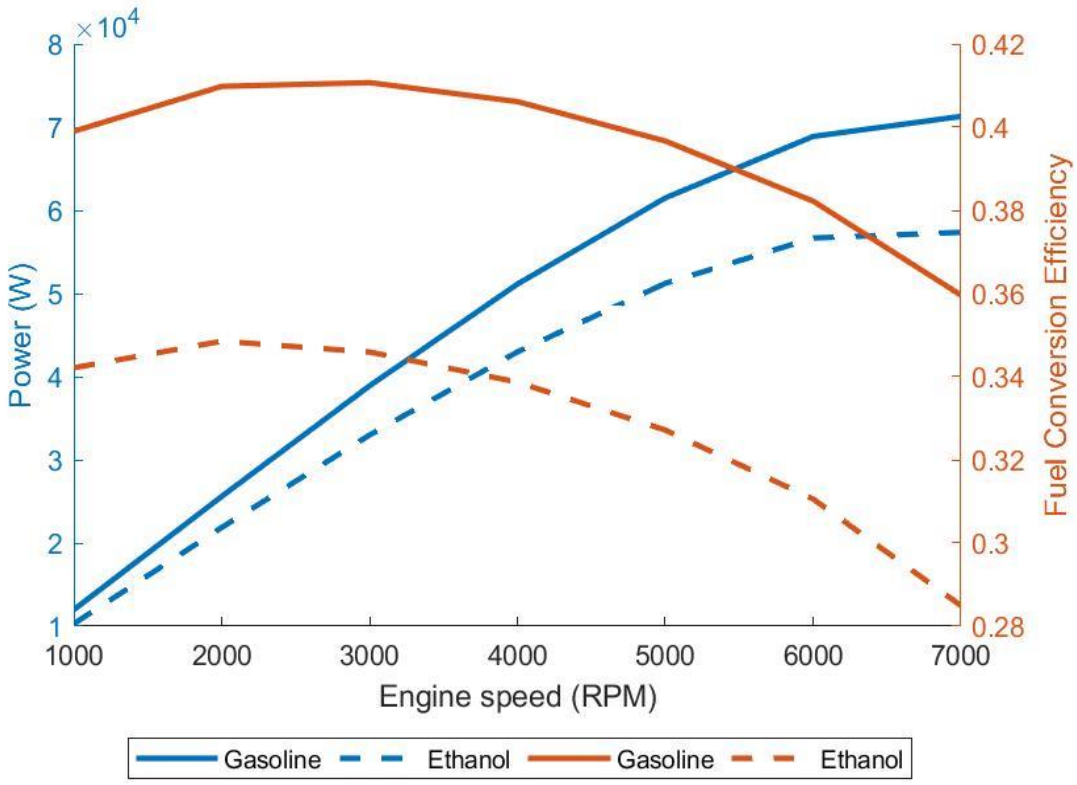

Figure 18: Evolution of engine power and fuel conversion efficiency with engine rotational speed (RPM) for gasoline and ethanol fuels at equivalence ratio 1.0 and 10.5 compression ratio.

7. CONCLUSIONS AND FUTURE WORK

The first conclusion of this work is that ICE will continue to be relevant in the short and medium term, having however to adapt to new emerging technologies such as electrical vehicles or incorporating new fuels (such as ethanol). The second conclusion is that energy system modelling is a way to improve its efficiency and reduce its GHG pollution either in its design or operation as it provides an underlying structure which is subject to testing and so improvement.

The third conclusion is that ICE models enable the study of new candidate renewable fuels as far as pollutant emissions, power production and conversion efficiency is concerned. The introduction of these new fuels contributes to mitigate the GHG problem. The fourth conclusion is that computational power is still evolving under Moore's law, computer interfaces are becoming more sophisticated and there is a wide supportive research community related to computation, which ensures computational models will contribute ever more to ICE efficiency.

The final conclusion is that credible detailed results were obtained of ICE operation. The results validate not only the methods used but also confirm ethanol as a viable ICE fuel.

As for future work, learning more about how ICE can cooperate with electric engines and more about new fuels is a goal. Learning advanced symbolic programming techniques to use exact mathematical derivation in modelling is another goal. Programming units should be able to make decisions so upgrading the programming units developed in this thesis to add decision making would be useful. Adding an experimental side to this ICE research, i.e. comparing modelling results with actual test bench engine results is mandatory. A final suggestion for future work would be to understand the market for ICE and so the marginal value of this type of research.

BIBLIOGRAPHY

1. *The Scope for improving the efficiency and environmental impact of internal combustion engines.* **LEACH, F.** 2020, Tramsportation Engineering 1.

2. *Potential and challenges for large scale application of biodiesel in automotive sector.* **AGAWAL, A.K., GUPTA, J.G. and DHAR, A.** 2017, Progress in Energy and Combustion Science 61, pp. 113-149.

3. *Stratified turbulent flames: Recent advances in understanding the influence of mixture inhomogeneities on premixed combustion and modeling challenges.* **LIAPUTNIKOV, A.N.** 2017, Progress in Energy and Combustion Science 62, pp. 87-132.

4. **HEYWOOD, John B.** *Internal Combustion Engine Fundamentals.* s.l. : McGraw-Hill, 1988.

5. *An Introduction to Combustion, Concepts and Applications.* **TURNS, S.R.** s.l. : Mc-Graw Hill, 2000.

6. **LAW, Chung K.** *Combustion Physics.* s.l. : Cambridge University Press, 2006.

7. **ONORATI, A and MONTENEGRO, G.** *1D and Multi-D Modeling Techniques for IC Engine Simulation.* s.l. : SAE International, 2020.

8. *Combustion and its Modeling in Spark-Ignition Engines.* **HEYWOOD, J.B.** s.l. : Comodia 94, 1994. International Symposium.

9. **ZELEZNIK, Frank J. and MCBRIDE, J.** *Modeling the Internal Combustion Engine.* s.l. : NASA Reference Publication 1094, 1985.

10. *Multi-Zone Quasi-Dimensional Combustion Models for Spark-Ignition Engines.* **CINELLA, P. et al.** 2013. Conference Paper in SAE Technical Papers.

11. **KAPRIELIAN, L.** *Modélisation 0D pour la combustion dans le moteurs à allumage commandé: dévelopments en proche paroi et dans le front de flamme.* École nationale supérieure d'arts et métiers - ENSAM. s.l. : Mécanique [physics.med.ph, 2015. phd thesis.

12. **BORDET, N.** *Modélisation 0D/1D de la combustion du diesel: du mode conventionnel au mode homogène.* s.l. : Université d´Órleans, 2011.

13. **LUM, Christopher.** [Online] 2020. https://www.youtube.com/user/christopherwlum.

14. **KESTIN, J.** *A course in Thermodynamics.* s.l. : CRC Press, 1979.

15. **SMITH, J.M. and VAN NESS, H.C.** *Introduction to Chemical Engineering Thermodynamics, 4th Edition.* s.l. : McGraw-Hill, 1987.

16. **BIRD, RR and LIGHTFOOT, EN.** *Transport Phenomena.* s.l. : John Wiley & Sons, 1960.

17. **LOOMIS, L and STERNBERG, S.** *Advanced Calculus.* s.l. : Jones and Bartlett Publishers, 1990.

18. *Measurement of laminar burning velocity of ethanol-air mixtures at elevated temperatures.* **KATOCH, A., MILLÁN-MERINO, A. and KUMAR, Sudarshan.** 2018, Fuel, Vol. 231, pp. 37-44.

19. **MCBRIDE, Bonnie J. and GORDON, S.** *Computer Program for Calculating and Fitting Thermodynamic Functions.* s.l. : NASA Reference Publication, 1271, November, 1992.

20. *A Method for Mass Burning Rate Calculation in Four Stroke Spark Ignition Internal Combustion Engines.* **CARVALHEIRA, Pedro.** Lisbon, Portugal : INEGI/FEUP, 22-26 July 2018. Proceedings IRF2018, 6th International Conference Integrity-reliability-future.

21. *Mixed halogenated dioxins/furans (PXDD/Fs) and biphenyls (PXBs) in food: Occurrence and toxic equivalent exposure using specific relative potencies.* **FERNANDES, A.R. and al, et.** 2014, Environment International, Vol. 73, pp. 104–110.

22. *Potentials and Challenges of Tailor-Made Fuels from Biomass.* **PISCHINGER, S. and MUETHER, M.** 2011, Energy Fuels, 25, pp. 4734–4744.

23. **MATHWORKS.** www.mathworks.com : s.n.

24. —. *Matlab: Symbolic Math Toolbox, a user´s guide. R2019b.* 2019.

25. —. *Simulink: Getting Started Guide.* s.l. : Mathworks, 2019.

26. *Computer Program for Calculating Properties of Equilibrium Combustion Products with Some Applications to I.C. Engines.* **OLIKARA, C and BORMAN, Gary L.A.** Detroit, Michigan : SAE, February 24-28, 1975. Automotive Engineering Congress and Exposition.

27. **SONIN, Ain A.** *The Physical Basis of Dimensional Analysis.* Department of Mechanical Engineering, MIT. Cambridge, MA : MIT, 2001.

28. *Simulation of fluid-flexible body interaction with heat transfer.* **P, GOON, et al.** 2017, International Journal of Heat and Mass Transfer, Vol. 410, pp. 20-33.

29. **BEECKMAN, J. RÖHL, et al.** *Laminar burning velocities and ignition delay times of ethanol.* Aachen, Germany : Institute for Combustion Technology, Shock Wave Laboratory. RWTH Aachen University.

30. **MATHWORKS.** *Modeling Guidelines for High-Integrity Systems.* s.l. : Mathworks, 2020.

31. *Solving CNLS problems using Levenberg-Marquardt algorithm :A new fitting strategy combining limits and a symbolic Jacobian matrix.* **ZIC, M, et al.** 2020, Journal of Electroanalytical Chemistry 866, p. 114171.

32. **MATHWORKS.** *Simulink: User's Guide.* s.l. : Mathworks, 2020.

33. *On Solving Ill Conditioned Linear Systems.* **DOUGLAS, C.C., LEE, L and YEUNG, M.C.** 2016, Procedia Computer Science, Volume 80, pp. 941-950.

34. *The Matlab ODE Suite.* **SHAMPINE, L.F. and REICHELT, Mark W.** No. 1, January 1997, SIAM J. Sci. Comput., Vol. Vol. 18, pp. 1-22.

35. *On the fractal basins of convergence of the libration points in the axisymmetric five-body problem: the Convex configuration.* **SURAJ, MS, et al.** 2019, International Journal of Non Linear Mechanics 109, pp. 80-106.

36. *Thermokarst in Siberian ice-rich permafrost: Comparison to asymmetric scalloped depression on Mars.* **ULRICH, M. et al.** 2010, Journal of Geophysical Research.

37. **MATHWORKS.** *MATLAB, the Language of Technical Computing. Version 6.* 2001.

38. —. MATLAB: Videos and Webinars. [Online] https://www.mathworks.com/videos/search.html?q=&page=1.

39. —. *Simulink: Modeling Guidelines for Code Generation.* s.l. : Mathworks, 2020.

40. —. *Simulink: Developing S Functions.* s.l. : Mathworks, 2020.

41. *Detecting Variability in MATLAB/Simulink Models: An Industry-Inspired technique and its Evaluations.* **SCHLIE, A. and WILLE, D.** September 2017. SPLC '17: Proceedings of the 21st International Systems and Software Product Line Conference. Vol. Volume A, pp. 215-224.

42. **MATHWORKS.** *Simulink: Reference.* s.l. : Mathworks, 2020.

43. —. Help Center. [Online] www.mathworks.com.

44. **MCKINTOSH, K.** *Lumps, Humps and Bumps: Three Detrimental Effects in the Current–Voltage.* s.l. : Centre for Photovoltaic Engineering, University of New South Wales, 2001. phd thesis.

45. *The Van der Waals Equation: analytical and approximate solutions.* **BERBERAN-SANTOS, M.N., BODUNOV, E.N. and POGLIANI, L.** May 2008, Journal of Mathematical Chemistry, Vol.43, nº 4.

46. **BUTTSWORTH, David R.** *Spark Ignition Internal Combustion Engine Modelling using Matlab.* s.l. : Faculty of Engineering & Surveying Technical Reports, October 16, 2002.

47. **COHEN, Richard E.** *Quantities, Units and Symbols in Physical Chemistry, Third Edition.* s.l. : IUPAC, 2007.

48. *Analysis of Piston, Connecting Rod and Crank Shaft assembly.* **GOPAL, G. et al.** 2017. Materials Today: Proceedings 4. pp. 7810-7819.

49. **HARIHARA, P. and CHILDS, D.** *Solving Problems in Dynamics and Vibrations Using MATLAB. Department of Mechanical Engineering, Texas A&M University, College Station.*

50. *Synthesis of Transportation Fuels from Biomass: Chemistry, Catalysts, and Engineering.* **HUBER, G.W., IBORRA, S and CORMA, A.** 2006, Chem. Rev. 106, pp. 4044-4098.

51. **KÉROMNÈS, A.** *Internal Combustion Engine Modeling.* s.l. : University of Burgundy, ISAT: Superior Institute for Automotive and Transports.

52. *Thermal Stress and Fatigue Analysis of Exhaust Manifold.* **YOON, S, LEE, S.B. and PARK, K.H.** 2004, Key Engineering Materials, Vols. 261-263, pp. 1203-1208.

53. *A Two-Zone Combustion Model for Knocking Prediction of Marine Natural Gas Engines.* **XIANG, La, SONG, E and DING, Yu.** 2018, Energies, Vol. 11, p. 561.

54. *An efficient power-flow approach based on Heun and King-Werner's methods for solving both well and ill-conditioned cases.* **TOSTADO-VELIZ, M., KAMEL, S. and JURDO, F.** 2020, Electrical Power and Energy Systems, Vol. 119, p. 105689.

55. *The effects of residual gas trapping on part load performance and emissions of a spark ignition direct injection engine fuelled with wet ethanol.* **LANZANOVA, T.D.M. et al.** 2019, Applied Energy 253, p. 113508.

56. **MATHWORKS.** *Simulink: Release Notes.* s.l. : Mathworks, 2020.

57. —. *Simulink: Graphical User Interface.* s.l. : Mathworks, 2020.

58. —. *MathWorks® Advisory Board Control Algorithm.* s.l. : Mathworks, 2020.

59. **SPITSOV, O.** *Heat Transfer Inside Internal Combustion Engine: Modelling and Comparison with Experimental Data.* 2013. Master's Thesis.

60. *General Method of Lyapunov Functionals Construction in Stability Investigations of Nonlinear Stochastic Difference Equations with Continuous Time.* **SHAIKET, L.** nº 2, 2005, Stochastics and Dynamics, Vol. Vol 5, pp. 175-188.

61. **NAGY, G.** *Ordinary Differential Equations.* Mathematics Department, Michigan State University. 2019.

62. *On the stability of fuzzy linear dynamical systems.* **NAJARIYAN, M and ZHAO, Y.** Journal of the Franklin Institute.

63. *Free-body diagram method for the uniqueness analysis of reactions and driving forces in redundantly constrained multibody systems with nonholomonic constraints.* **PEKAL, M., WOJTYRA, M. and FRACZEK, J.** 2019, Mechanism and Machine Theory, Vol. 133, pp. 329-346.

64. *Piston geometry effects in a light duty, swirl supported diesel engine: Flow structure characterization.* **PERINI, F. et al.** 2018, International Journal of Engine Research, Vol. 19 (10), pp. 1079-1098.

65. *A 2-zone Combustion Model and its Validation for a Spark Ignition Engine Fueled with Coal-Bed Gas.* **QIAN, Y., HONGLAN, G and HONGMING, Xu.** HKIE Transactions 16.2, pp. 28-37.

ANNEX A

Mathematical Model of Simulation of the Four-Stroke Spark Ignition Engine Cycle

Table 5: Mass Matrix indexing: Intake-Compression phase

i	Variable		i	Variable
1	p		10	$m_{\mathrm{O},u}$
2	V_u		11	$m_{\mathrm{OH},u}$
3	$m_{\mathrm{CO_2},u}$		12	$m_{\mathrm{NO},u}$
4	$m_{\mathrm{H_2O},u}$		13	$m_{\mathrm{Ar},u}$
5	$m_{\mathrm{N_2},u}$		14	$m_{f,u}$
6	$m_{\mathrm{O_2},u}$		15	T_u
7	$m_{\mathrm{CO},u}$		16	$m_{\mathrm{col,adm}}$
8	$m_{\mathrm{H_2},u}$		17	$knock$
9	$m_{\mathrm{H},u}$			

Table 6: Mass Matrix indexing: Combustion phase

i	Variable		i	Variable		i	Variable
1	p		16	T_u		31	$x_{\mathrm{H_2O},b}$
2	V_u		17	V_b		32	$x_{\mathrm{N_2},b}$
3	$m_{\mathrm{CO_2},u}$		18	$m_{\mathrm{CO_2},b}$		33	$x_{\mathrm{O_2},b}$
4	$m_{\mathrm{H_2O},u}$		19	$m_{\mathrm{H_2O},b}$		34	$x_{\mathrm{CO},b}$
5	$m_{\mathrm{N_2},u}$		20	$m_{\mathrm{N_2},b}$		35	$x_{\mathrm{H_2},b}$
6	$m_{\mathrm{O_2},u}$		21	$m_{\mathrm{O_2},b}$		36	$x_{\mathrm{H},b}$
7	$m_{\mathrm{CO},u}$		22	$m_{\mathrm{CO},b}$		37	$x_{\mathrm{O},b}$
8	$m_{\mathrm{H_2},u}$		23	$m_{\mathrm{H_2},b}$		38	$x_{\mathrm{OH},b}$
9	$m_{\mathrm{H},u}$		24	$m_{\mathrm{H},b}$		39	$x_{\mathrm{NO},b}$
10	$m_{\mathrm{O},u}$		25	$m_{\mathrm{O},b}$		40	$x_{\mathrm{Ar},b}$
11	$m_{\mathrm{OH},u}$		26	$m_{\mathrm{OH},b}$		41	$x_{\mathrm{N},b}$
12	$m_{\mathrm{NO},u}$		27	$m_{\mathrm{NO},b}$		42	T_b
13	$m_{\mathrm{Ar},u}$		28	$m_{\mathrm{Ar},b}$		43	r_b
14	$m_{\mathrm{N},u}$		29	$m_{\mathrm{N},b}$		44	n_{lk}
15	$m_{f,u}$		30	$x_{\mathrm{CO_2},b}$		45	$knock$

Table 7: Mass Matrix indexing: Expansion Exhaust phase

i	Variable		i	Variable
1	p		9	$m_{\mathrm{H},b}$
2	V_b		10	$m_{\mathrm{O},b}$
3	$m_{\mathrm{CO_2},b}$		11	$m_{\mathrm{OH},b}$
4	$m_{\mathrm{H_2O},b}$		12	$m_{\mathrm{NO},b}$
5	$m_{\mathrm{N_2},b}$		13	$m_{\mathrm{Ar},b}$
6	$m_{\mathrm{O_2},b}$		14	$m_{\mathrm{N},b}$
7	$m_{\mathrm{CO},b}$		15	T_b
8	$m_{\mathrm{H_2},b}$			

Table 8: Mass Matrix indexing: Crossflow BTDC phase

i	Variable		i	Variable
1	p		9	$m_{\mathrm{H},b}$
2	V_b		10	$m_{\mathrm{O},b}$
3	$m_{\mathrm{CO_2},b}$		11	$m_{\mathrm{OH},b}$
4	$m_{\mathrm{H_2O},b}$		12	$m_{\mathrm{NO},b}$
5	$m_{\mathrm{N_2},b}$		13	$m_{\mathrm{Ar},b}$
6	$m_{\mathrm{O_2},b}$		14	$m_{f,b}$
7	$m_{\mathrm{CO},b}$		15	T_b
8	$m_{\mathrm{H_2},b}$		16	$m_{\mathrm{col,adm}}$

Table 9: Mass Matrix indexing: Crossflow ATDC phase

i	Variable		i	Variable
1	p		10	$m_{\mathrm{O},u}$
2	V_u		11	$m_{\mathrm{OH},u}$
3	$m_{\mathrm{CO_2},u}$		12	$m_{\mathrm{NO},u}$
4	$m_{\mathrm{H_2O},u}$		13	$m_{\mathrm{Ar},u}$
5	$m_{\mathrm{N_2},u}$		14	$m_{f,u}$
6	$m_{\mathrm{O_2},u}$		15	T_u
7	$m_{\mathrm{CO},u}$		16	$m_{\mathrm{col,adm}}$
8	$m_{\mathrm{H_2},u}$		17	*knock*
9	$m_{\mathrm{H},u}$			

ANNEX B

Program Listing:

A: Engine.m: the main program:

- organized from alfa to part I, II, … Sections a. b. c to d. e. f.
- ~2,500 lines of code.
- can be run from data files.
- coordinates other programs.
- contains iterative scheme

B: comb.m: program simulating combustion stage.

C: intakecomp.m: program simulating intake and compression stage.

D: expexh.m: program simulating expansion and exhaust stage.

E: crossflowBTDC.m: program simulating crossflow BTDC stage.

F: crossflowATDC.m: program simulating crossflowATDC stage.

G: MassBalance.m: program capable of performing symbolic derivatives.

H: Results.m: collection of programs that produce model results: temperature, mole fractions, mass.

I: ecp.m: auxiliary program.

J: fueldata.m: auxiliary data base.

K: Auxiliary functions: functions designed for specific tasks.

Other.